Synthesis of a series of new platinum organometallic complexes derived from bidentate Schiff-base ligands and their catalytic activity in the hydrogenative and dehydrogenative silylation of alkenes.

M. Belhadj Lachachi,[a,b] Tayeb Benabdallah,[b] Pedro M. Aguiar,[a] M. Hadj Youcef,[b] Adrian C. Whitwood[a] and Jason M. Lynam[a].

[a] Department of Chemistry, University of York, Heslington, York, YO10 5DD, UK.
[b] Laboratory of Chemistry and Electrochemistry of Metallic Complexes, Department of Organic Chemistry, Faculty of Chemistry, University of Sciences and Technology of Oran, BP 1505 El M'Naouar, Oran, 31000, Algeria.

Supporting Information

S1. Spectroscopic Information **S3**

S1.1. UV-Vis spectroscopy for the five Schiff base ligands S3

S2. Crystallographic Information **S7**

S2.1. General Details S7

S2.2. Details of the data collection and structure refinement S8

S3. Mass Spectra **S10**

S3.1. ESI Mass spectrum of complex **4a** S10

S3.2. ESI Mass spectrum of complex **4b** S11

S3.3. ESI Mass spectrum of complex **4c** S12

S3.4. ESI Mass spectrum of complex **4d** S13

S3.5. LIFDI Mass spectrum of complex **4e** S14

S4. NMR Spectra **S15**

S4.1. Solid state ^{1}H NMR spectra of **3a**-**3e** S15

S4.2. ^{13}C{^{1}H}CPMAS NMR spectrum of **3a**-**3e** S16

S4.3. ^{13}C{^{1}H}CPMAS NMR spectrum of **3a** S17

S4.4. Expansion of ^{13}C{^{1}H}CPMAS NMR spectrum of **3a** S18

S4.5. ^{13}C{^{1}H}CPMAS NMR spectrum of **3b** S19

S4.6. Expansion of ^{13}C{^{1}H}CPMAS NMR spectrum of **3b** S20

S4.7. ^{13}C{^{1}H}CPMAS NMR spectrum of **3c** S21

S4.8. Expansion of ^{13}C{^{1}H}CPMAS NMR spectrum of **3c** S22

S4.9. ^{13}C{^{1}H}CPMAS NMR spectrum of **3d** S23

S4.10. ^{13}C{^{1}H}CPMAS NMR spectrum of **3e** S24

S4.11. Extension of ^{13}C{^{1}H}CPMAS NMR spectrum of 3e S25

S4.12. ^{1}H NMR spectrum of 3a from the reaction of **1** with **2a** S26

S4.13. ^{13}C NMR spectrum of 3a from the reaction of **1** with **2a** S27

S4.14. ^{1}H NMR spectrum of 3b from the reaction of **1** with **2b** S28

S4.15. ^{13}C NMR spectrum of 3b from the reaction of **1** with **2b** S29

S4.16. ^{1}H NMR spectrum of 3c from the reaction of **1** with **2c** S30

S4.17. ^{13}C NMR spectrum of 3c from the reaction of **1** with **2c** S31

S4.18. ^{1}H NMR spectrum of 3d from the reaction of **1** with **2d** S32

S4.19. ^{13}C NMR spectrum of 3d from the reaction of **1** with **2d** S33

S4.20. ^{1}H NMR spectrum of 3e from the reaction of **1** with **2e** S34

S4.21. ^{13}C NMR spectrum of 3e from the reaction of **1** with **2e** S35

S4.22. ^{1}H NMR spectrum of **4b-a** and **4b-b** S36
S4.23. ^{13}C NMR spectrum of **4b-a** and **4b-b** S37
S4.24. ^{1}H NMR spectrum of **4c-a** and **4c-b** S38
S4.25. ^{13}C NMR spectrum of **4c-a** and **4c-b** S40
S4.26. ^{1}H NMR spectrum of **4d-a** and **4d-b** S41
S4.27. ^{1}H NMR spectrum of **4e-a** and **4e-b** S43
S4.28. ^{13}C NMR spectrum of **4e-a** and **4e-b** S45
S5. References **S46**

S1. Spectroscopic Information

S1.1. UV-Vis spectroscopy for the five Schiff base ligands

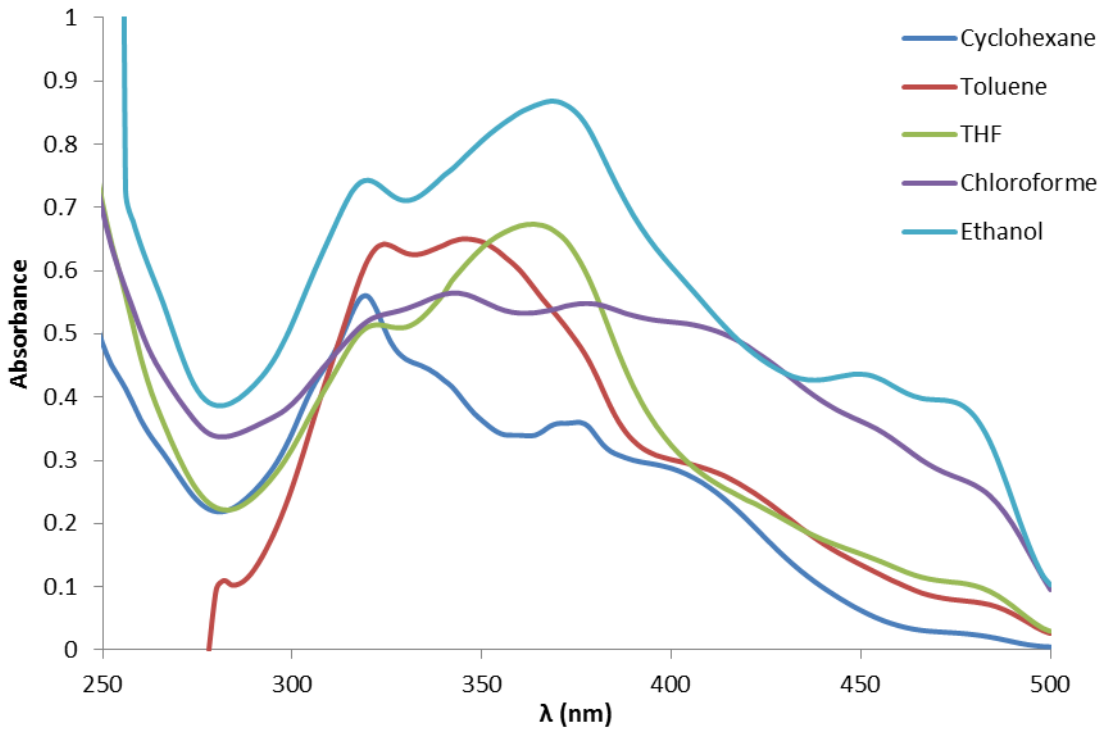

Fig. S1 *UV-VIS Spectra of* ***3a*** *in different solvants*

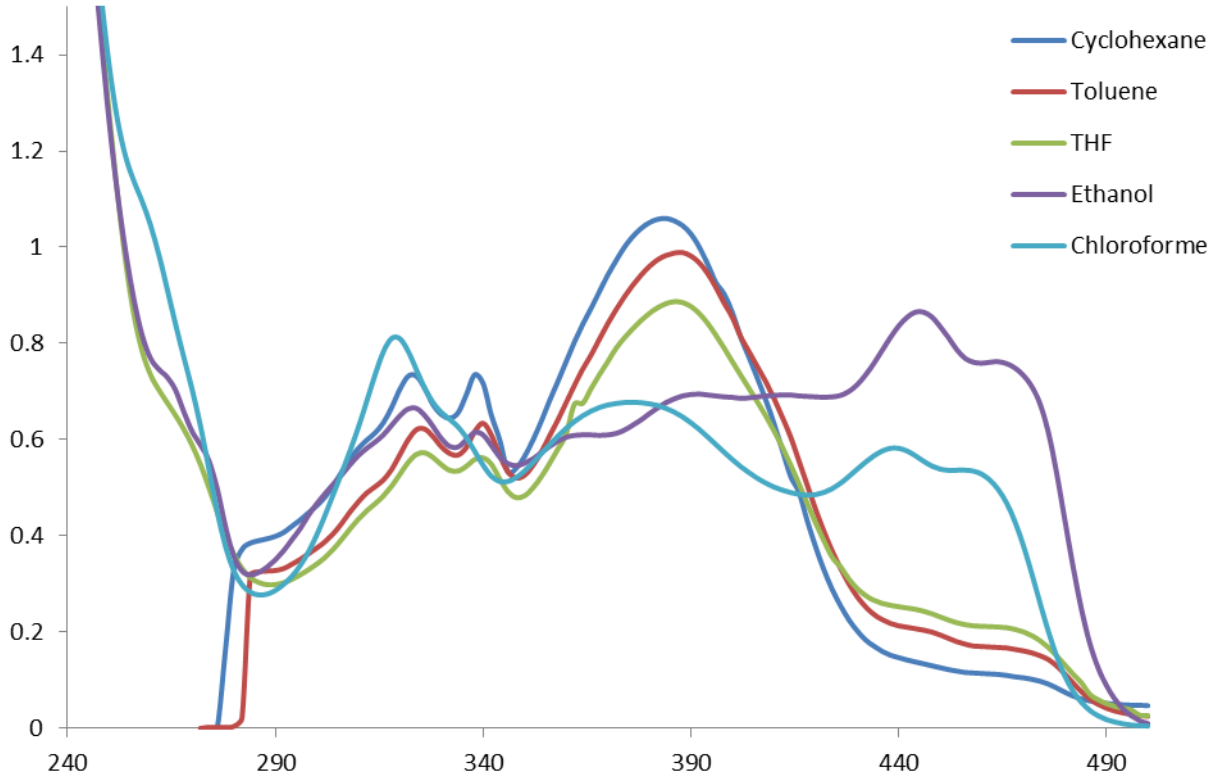

Fig.S2 *UV-VIS Spectra of* ***3b*** *in different solvants*

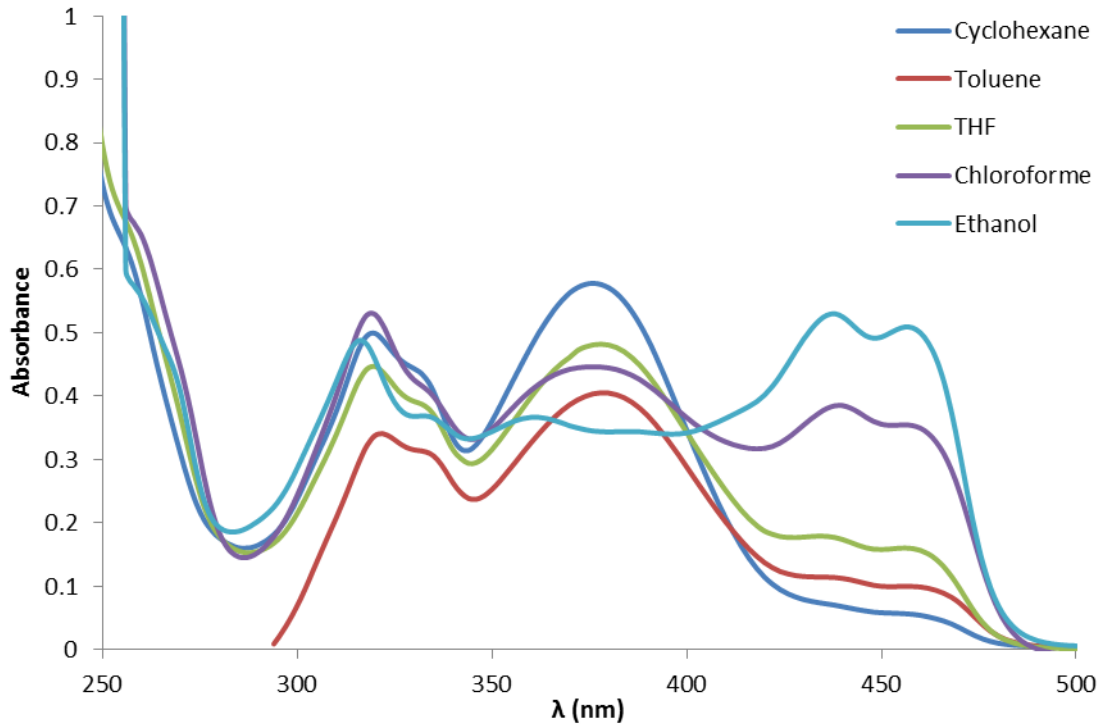

Fig. S3 *UV-VIS Spectra of* ***3c*** *in different solvants*

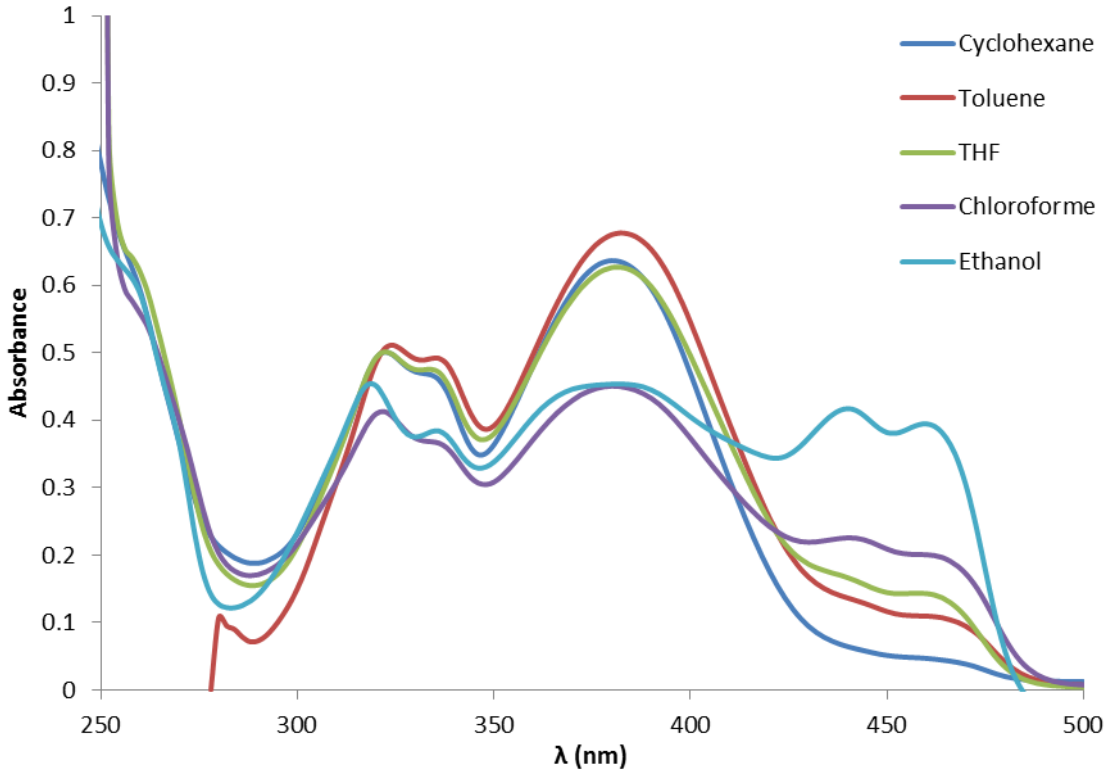

Fig. S4 *UV-VIS Spectra of* ***3d*** *in different solvants*

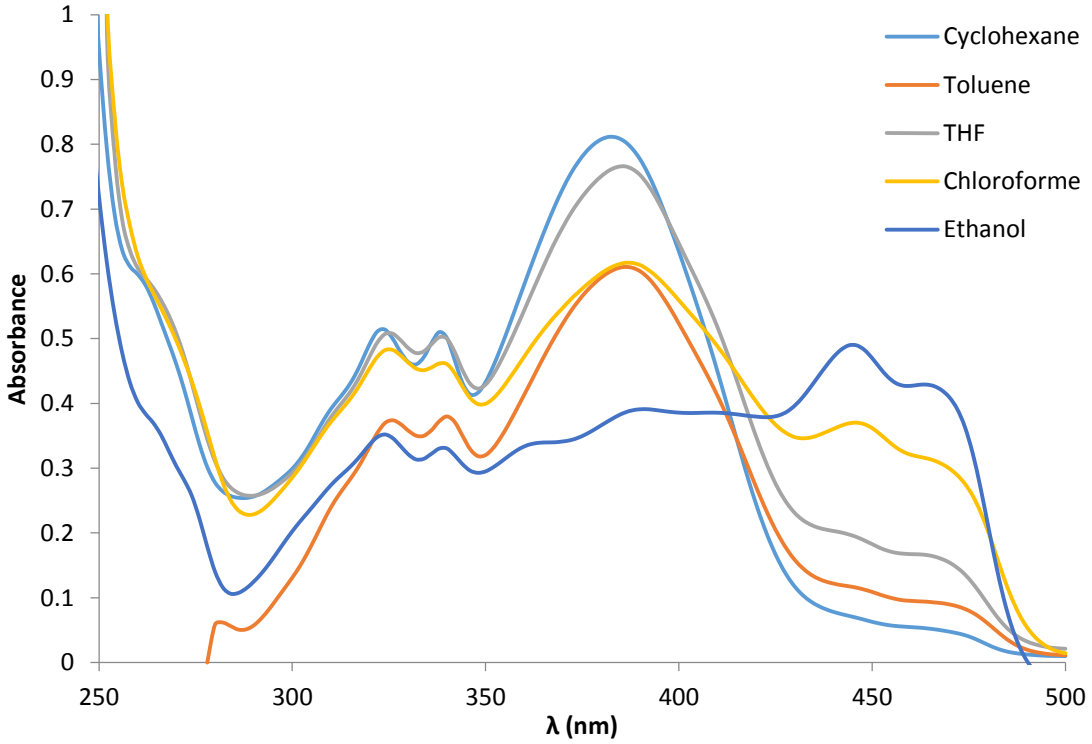

Fig. S5 *UV-VIS Spectra of* ***3e*** *in different solvants*

Table 1 Wavelengths and molar extinction coefficients of absorption electronic bands for the five *Schiff* bases in different solvents. [s] shoulder.

Solvent	λ / nm, ε / $dm^{-3}mol^{-1}cm^{-1}$				
	3a	***3b***	***3c***	***3d***	***3e***
Cyclohexane	480[s], 454[s]	472[s], 440[s]	460[s] , 440[s]	468[s], 442[s]	466[s], 442[s]
	402[s]	384 (2.22×10^4)	376 (1.16×10^4)	380 (1.27×10^4	382 (1.62×10^4)
	376 (7.18×10^3)	338 (1.47×10^4)	330[s]	338[s]	338 (1.02×10^4)
	338[s]	322 (1.40×10^4)	320 (6.76×10^3)	322 (1.0×10^4)	324 (1.03×10^4)
	320 (1.12×10^4)				
Toluene	484[s], 456[s]	474[s], 450[s]	460[s], 440[s]	466[s], 444[s]	464[s], 442[s]
	418[s]	388 (1.98×10^4)	378 (8.10×10^3)	382 (1.36×10^4)	386 (1.22×10^4)
	346 (1.30×10^4)	340 (1.27×10^4)	332[s]	336 (9.84×10^3)	340 (7.60×10^3)
	324 (1.28×10^4)	326 (1.24×10^4)		324 (1.02×10^4)	326 (7.48×10^3)
	278 (4.68×10^4)				
THF	482[s], 452[s]	472[s], 448[s]	456[s], 434[s]	462[s], 440[s]	462[s], 440[s]
	364 (1.35×10^4)	386 (1.71×10^4)	378 (9.64×10^3)	382 (1.25×10^4)	386 (1.53×10^4)
	322 (1.03×10^4)	340 (1.06×10^4)	326[e]	334 (9.51×10^3)	338 (1.00×10^4)
		326 (1.09×10^4)	320 (8.93×10^3)	322 (1.00×10^4)	326 (1.02×10^4)
Chloroform	478[s], 454[s]	464[s]	456 (7.09×10^3)	464[s]	464[s]
	404[s]	448 (7.86×10^3)	438 (7.69×10^3)	440 (4.51×10^3)	446 (7.41×10^3)
	378 (1.10×10^4)	388 (9.20×10^3)	376 (8.92×10^3)	380 (9.01×10^3)	386 (1.23×10^4)
	342 (1.13×10^4)	340 (7.24×10^3)	330[s]	334 (7.37×10^3)	338 (9.23×10^3)
		324 (7.86×10^3)	318 (1.06×10^4)	322 (8.26×10^3)	326 (9.65×10^3)
Ethanol	472s, 450s	464[s]	456 (1.02×10^4)	460 (7.89×10^3)	464 (8.58) $\times 10^3$
	372 (1.52×10^4)	444 (1.73×10^4)	438 (1.06×10^4)	440 (8.35×10^3)	444 (9.79×10^3)
	320 (1.25×10^4)	392 (1.39×10^4)	362 (7.33×10^3)	382 (9.07×10^3)	392 (7.82×10^3)
		338 (1.23×10^4)	332 (7.37×10^3)	336 (7.68×10^3)	360[s]
		322 (1.33×10^4)	316 (9.76×10^3)	318 (9.05×10^3)	340 (6.61×10^3)
					324 (7.04×10^3)

S2. Crystallographic Information

S2.1. General Details

Diffraction data for **3a**, **3c**, **3d** and **4c** were collected at 110 K on an Oxford Diffraction SuperNova diffractometer with Mo-K_α radiation (λ = 0.71073 Å) using an EOS CCD camera. The crystal was cooled with an Oxford Instruments Cryojet. Diffractometer control, data collection, initial unit cell determination, frame integration and unit-cell refinement was carried out with "Crysalis".[1] Face-indexed absorption corrections were applied using spherical harmonics, implemented in SCALE3 ABSPACK scaling algorithm.[2] OLEX2[3] was used for overall structure solution, refinement and publication data. Within OLEX2[3] the algorithm used for structure solution was Superflip,[4a,4b,4c] except for **3a** which used the direct methods algorithm in SHELXS,[5] refinement was performed by full-matrix least-squares using SHELXL-97.[5] All non-hydrogen atoms were refined anisotropically. Hydrogen atoms were placed using a "riding model" and included in the refinement at calculated positions.

S2.2. Details of the data collection and structure refinement

Compound	**3a**	**3c**	**3d**
CCDC	1055267	1055268	1055269
Empirical formula	$C_{17}H_{12}N_2O_3$	$C_{17}H_{13}NO$	$C_{17}H_{12}ClNO$
Formula weight	292.29	247.28	281.68
Temperature / K	110.00(10)	110.05(10)	110.1(2)
Crystal system	monoclinic	monoclinic	monoclinic
Space group	$P2_1/c$	P-2	$P2_1/n$
a / Å	8.0204(2)	11.9893(2)	4.69799(14)
b / Å	12.7917(3)	14.0266(3)	20.2659(8)
c / Å	13.0855(4)	7.25469(15)	13.4966(4)
α/°	90.00	90	90.00
β/°	98.087(3)	90.2237(18)	93.830(3)
γ/°	90.00	90	90.00
Volume / $Å^3$	1329.15(6)	1220.01(4)	1282.13(8)
Z	4	4	4
ρ_{calc} / mg mm^{-3}	1.461	1.346	1.459
μ / mm^{-1}	0.102	0.084	0.291
F(000)	608.0	520.0	584.0
Crystal size / mm^3	0.2591 × 0.1209 × 0.0853	0.2242 × 0.165 × 0.0836	0.9556 × 0.1145 × 0.1095
2Θ range for data collection / °	6.04 to 60.06°	5.802 to 64.17°	6.06 to 64.5°
Index ranges	-11 ≤ h ≤ 11 -18 ≤ k ≤ 18, -17 ≤ l ≤ 18	-17 ≤ h ≤ 17 -20 ≤ k ≤ 17 -10 ≤ l ≤ 9	-5 ≤ h ≤ 6, -29 ≤ k ≤ 28, -13 ≤ l ≤ 19
Reflections collected	12067	8635	7137
Independent reflections	3892[R(int) = 0.0253]	3754 [R_{int} = 0.0234]	4078[R(int) = 0.0214]
Data/restraints/parameters	3892/0/203	3754/0/176	4078/0/191
Goodness-of-fit on F^2	1.073	1.032	1.051
Final R indexes [I>2σ (I)]	R_1 = 0.0441, wR_2 = 0.1245	R_1 = 0.0464 wR_2 = 0.1196	R_1 = 0.0409, wR_2 = 0.0980
Final R indexes [all data]	R_1 = 0.0512, wR_2 = 0.1302	R_1 = 0.0584 wR_2 = 0.1285	R_1 = 0.0493, wR_2 = 0.1046
Largest diff. peak/hole / e $Å^{-3}$	0.39/-0.29	0.39/-0.23	0.48/-0.24

Table S1 Details of the data collection and structure refinement for X-ray structure determinations of ligands.

Compound	**4c**	[**6e**]
CCDC Code	1055270	1055271
Empirical formula	$C_{25}H_{25}NO_2Pt$	$C_{54.5}H_{58}N_2O_5Pt_2$
Formula weight	566.55	1211.21
Temperature / K	110.05(10)	110.00(10)
Crystal system	triclinic	triclinic
Space group	P-1	P-1
a / Å	9.5684(5)	7.1629(4)
b / Å	10.2961(5)	17.1325(7)
c / Å	12.1674(7)	19.9614(8)
α/°	98.042(4)	87.663(3)
β/°	112.189(5)	84.731(4)
γ/°	109.089(5)	82.141(4)
Volume / $Å^3$	1000.24(10)	2415.37(4)
Z	2	2
ρ_{calc} / mg mm^{-3}	1.881	1.665
μ / mm^{-1}	7.036	5.835
F(000)	552.0	1190.0
Crystal size / mm^3	0.1037 × 0.0527 × 0.0135	0.3379 × 0.1045 × 0.0492
2Θ range for data collection / °	5.786 to 50.694°	5.764 to 60.272°
Index ranges	-11 ≤ h ≤ 11 -12 ≤ k ≤ 11 -14 ≤ l ≤ 14	-9≤ h ≤ 9 -23 ≤ k ≤ 23 -26 ≤ l ≤ 27
Reflections collected	6482	19471
Independent reflections	3660 [R_{int} = 0.0342, R_{sigma} = 0.0607]	12298 [R_{int} = 0.0282, R_{sigma}= 0.0588]
Data/restraints/parameters	3660/60/298	12298/6/593
Goodness-of-fit on F^2	1.049	1.046
Final R indexes [I>2σ (I)]	R_1 = 0.0326, wR_2 = 0.0585	R_1 = 0.0353 wR_2 = 0.0753
Final R indexes [all data]	R_1 = 0.0377, wR_2 = 0.0601	R_1 = 0.0533 wR_2 = 0.0812
Largest diff. peak/hole / e $Å^{-3}$	1.44/-0.81	2.45/-1.96

Table S1 Details of the data collection and structure refinement for X-ray structure determinations of ligands.

S3. Mass Spectra

S3.1. ESI Mass spectrum of complex 4a

L1-PtCOD

York - Chemistry - Mass Spectrometry Service Report

Analysis Information

Acquisition Date 22/04/2013 14:30:12

Analysis Filename	jml41029bl_1-b,5_01_44280.d
Method	800p_meoh.m
Submission Name	jml41029bl
Instrument	micrOTOF
ESI	Positive

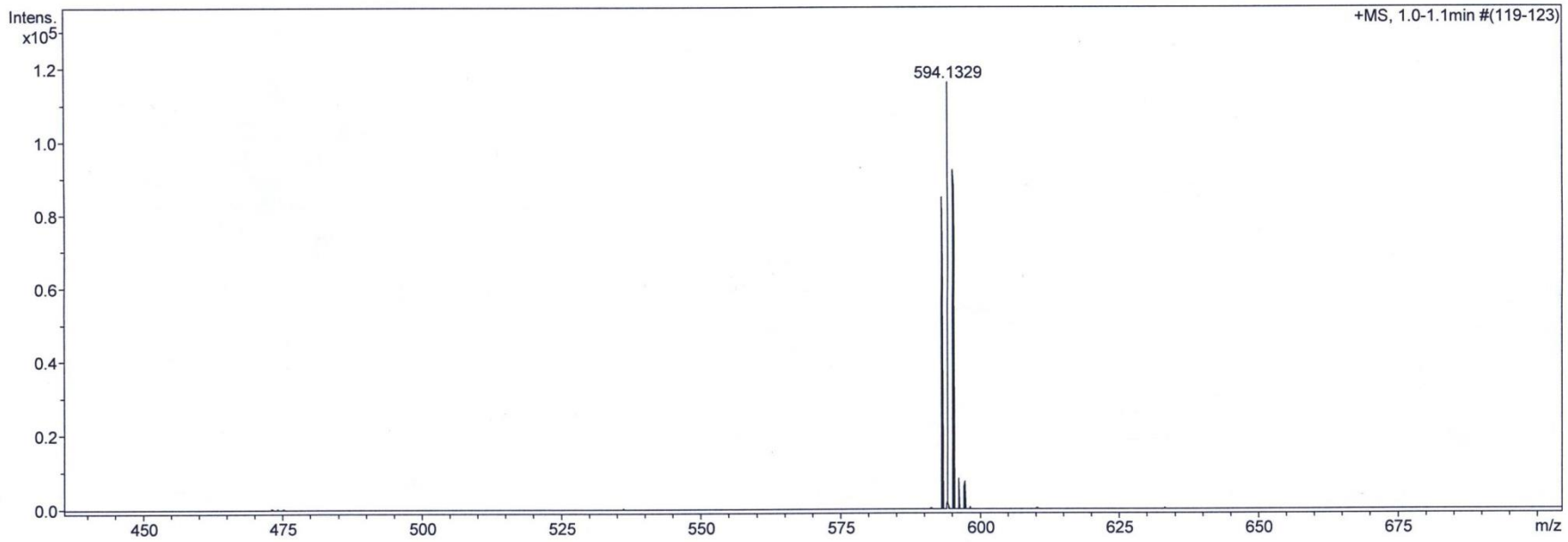

Meas. m/z	#	Formula	m/z	err [ppm]	err [mDa]	mSigma	Mean err [ppm]
594.1329	1	C 25 H 23 N 2 O 3 Pt	594.1353	3.7	2.2	65.6	3.8

S3.2. ESI Mass spectrum of complex 4b

PtL2COD

York - Chemistry - Mass Spectrometry Service Report

Analysis Information

Acquisition Date 25/04/2013 14:26:57

Analysis Filename	jml41110bl_1-e,3_01_44409.d
Method	800p_meoh.m
Submission Name	jml41110bl
Instrument	micrOTOF
ESI	Positive

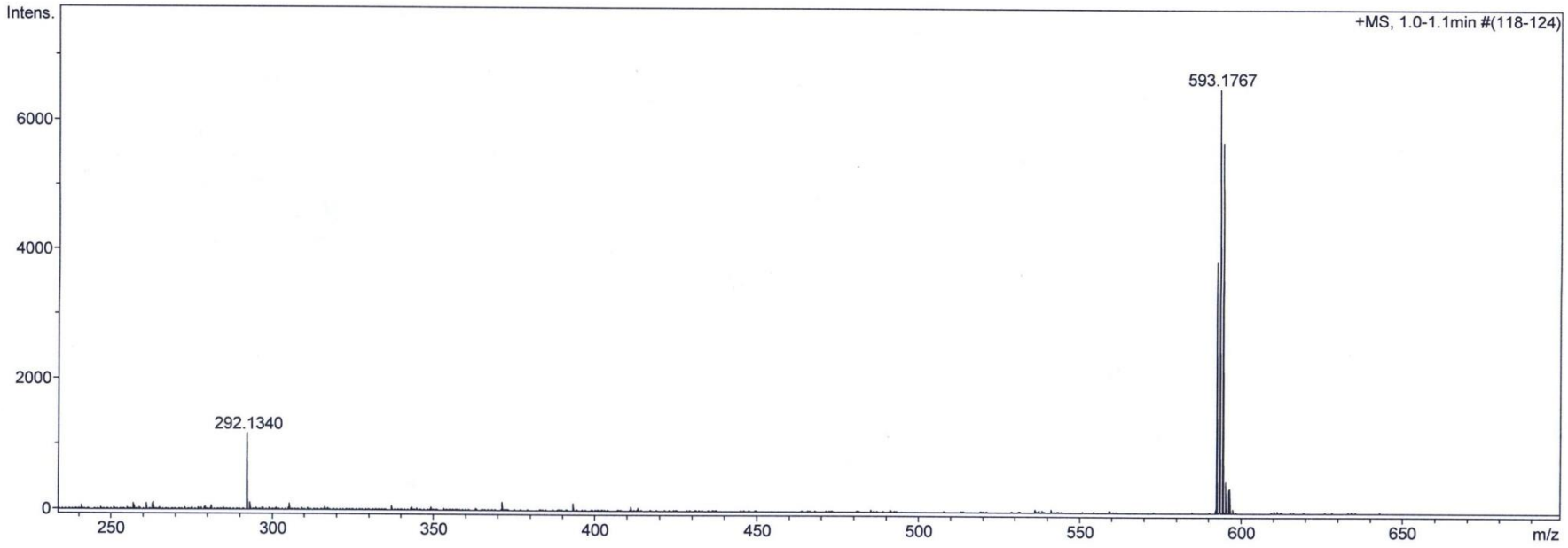

Meas. m/z	#	Formula	m/z	err [ppm]	err [mDa]	mSigma	Mean err [ppm]
593.1767	1	C 27 H 28 N O 2 Pt	593.1765	-0.4	-0.2	112.5	-1.8

S3.3. ESI Mass spectrum of complex 4c

PtL3 COD

York - Chemistry - Mass Spectrometry Service Report

Analysis Information

Acquisition Date 17/10/2014 12:33:56

Analysis Filename	jml48804bl_P1-B-9_01_54125.d
Method	800p_meoh1260_2c1s.m
Submission Name	jml48804bl
Instrument	micrOTOF
ESI	Positive

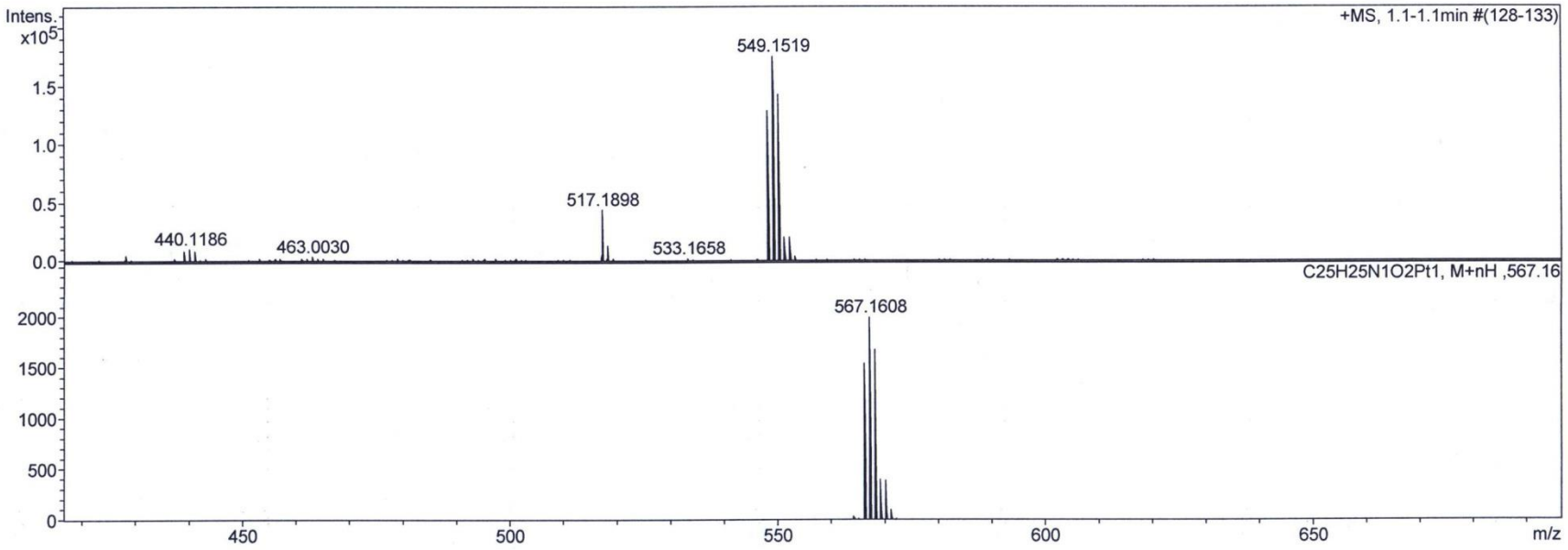

Meas. m/z	#	Formula	m/z	err [ppm]	err [mDa]	mSigma	Mean err [ppm]
549.1519	1	C 25 H 24 N O Pt	549.1503	-3.0	-1.6	37.0	-3.6

S3.4. ESI Mass spectrum of complex 4d

L4 PtCOD

York - Chemistry - Mass Spectrometry Service Report

Analysis Information

Acquisition Date 22/04/2013 14:26:34

Analysis Filename	jml41028bl_1-b,4_01_44279.d
Method	800p_meoh.m
Submission Name	jml41028bl
Instrument	micrOTOF
ESI	Positive

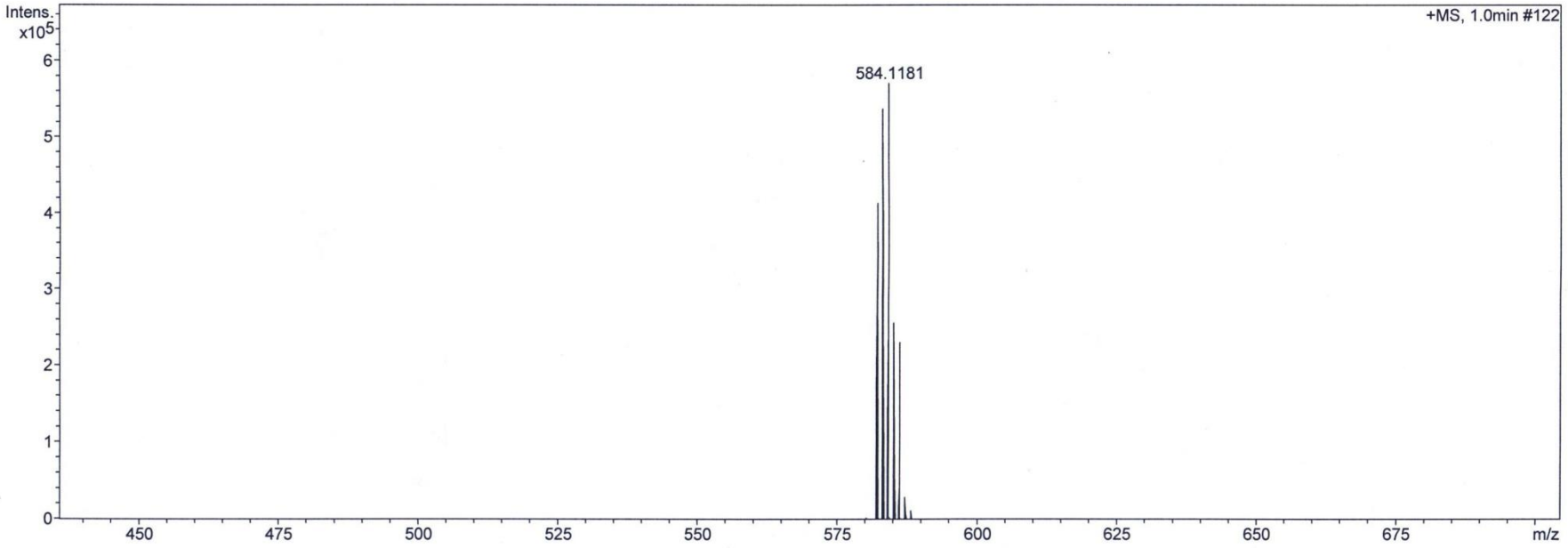

Meas. m/z	#	Formula	m/z	err [ppm]	err [mDa]	mSigma	Mean err [ppm]
584.1181	1	C 25 H 24 Cl N O Pt	584.1191	1.2	0.7	320.9	-0.2

S3.5. LIFDI Mass spectrum of complex 4e

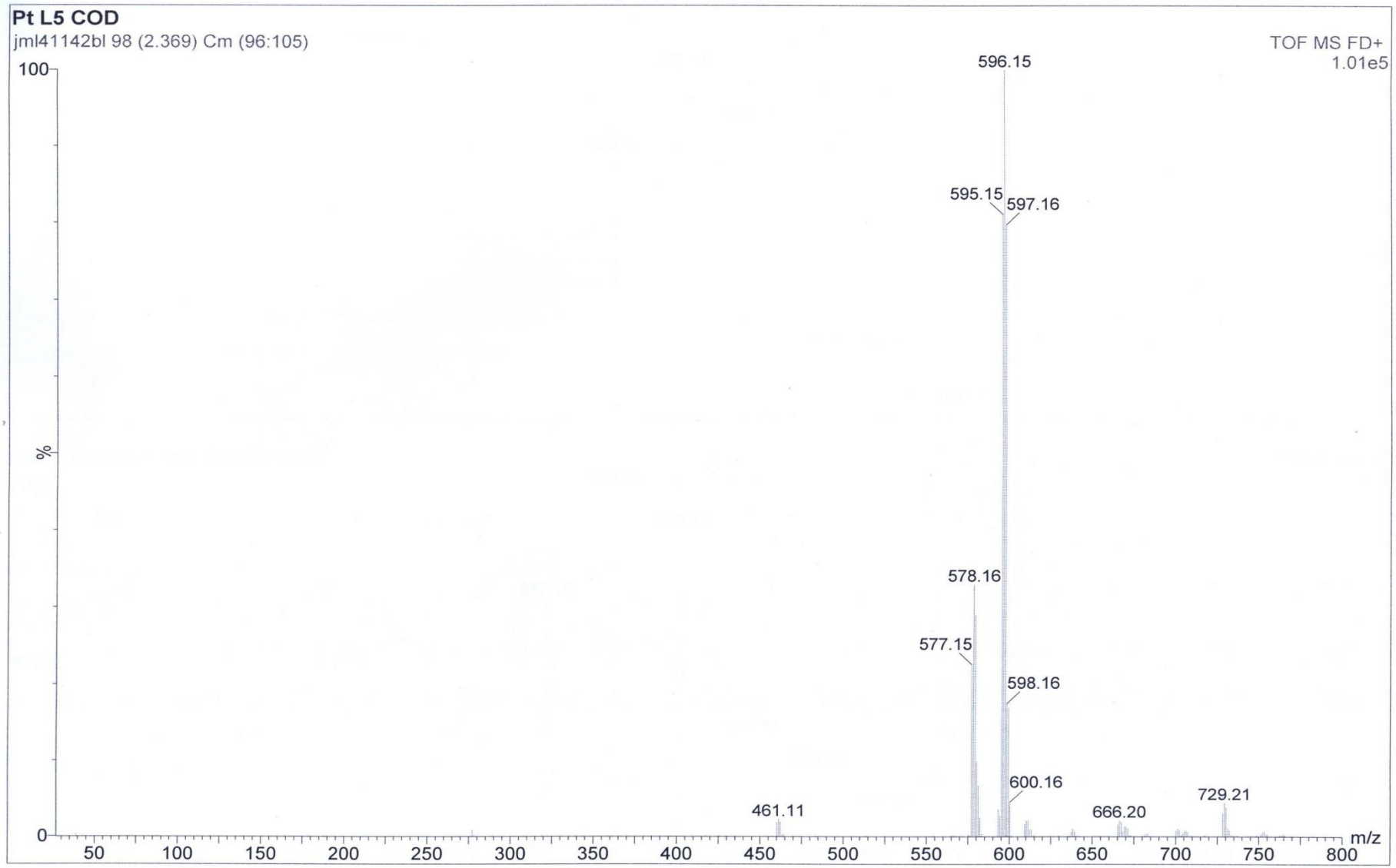

S4. NMR Spectra

S4.1. Solid state ^{1}H NMR spectra of 3a-3e

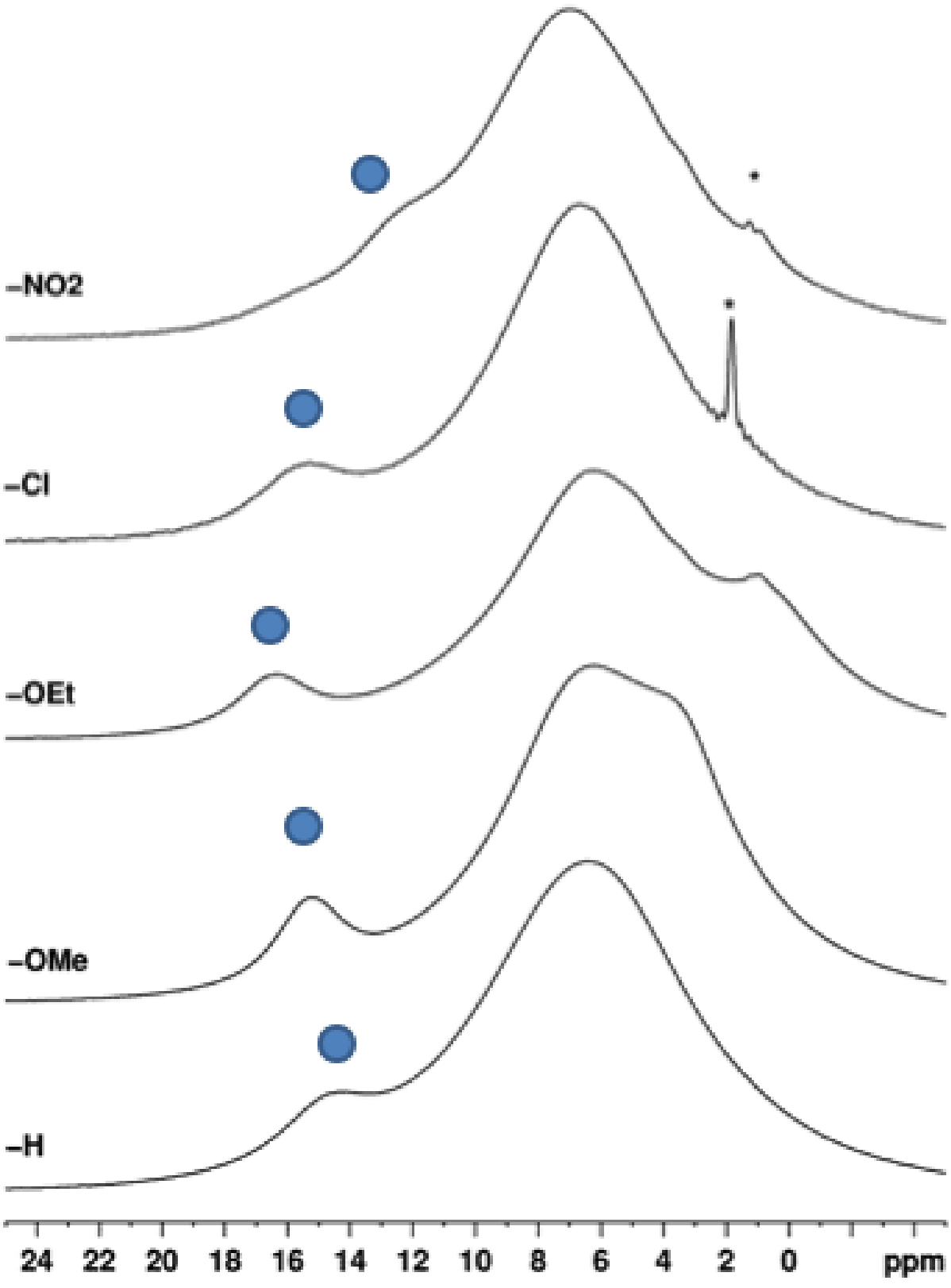

S4.2. $^{13}C\{^{1}H\}$CPMAS NMR spectrum of 3a-3e

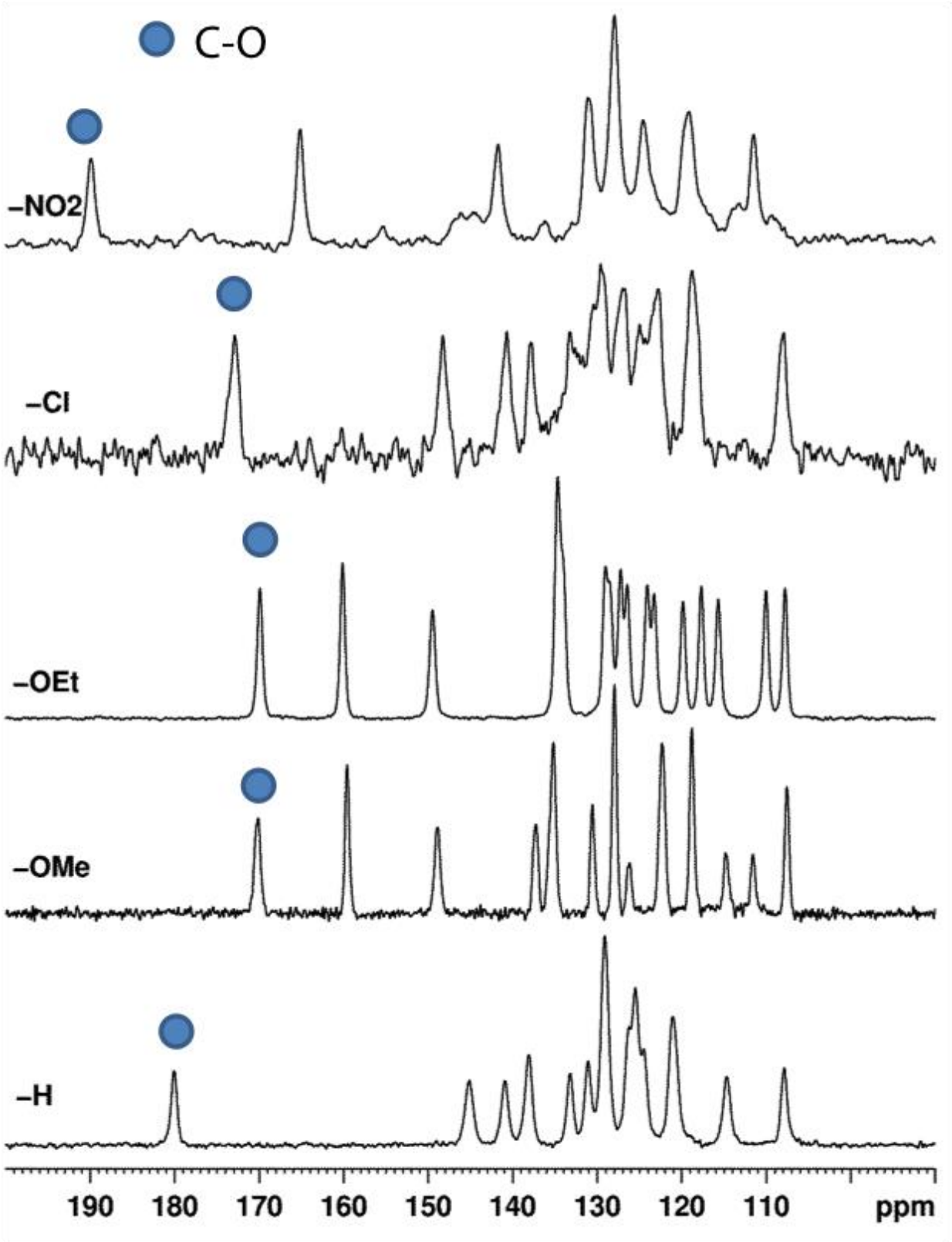

S4.3. $^{13}C\{^{1}H\}$CPMAS NMR spectrum of 3a

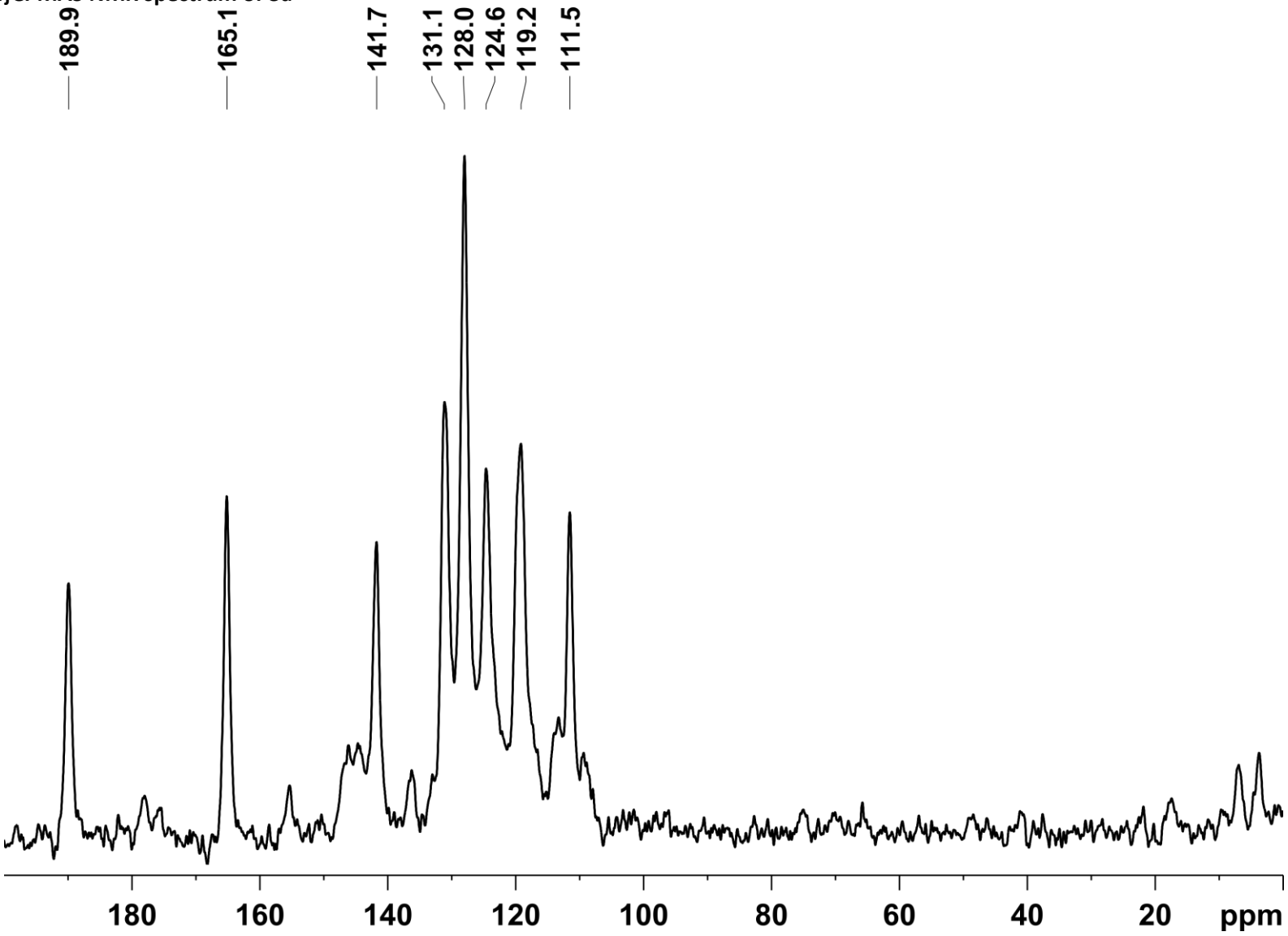

S4.4. Expansion of $^{13}C\{^{1}H\}$CPMAS NMR spectrum of 3a

With normal CP and dipolar dephasing (CP-DD)

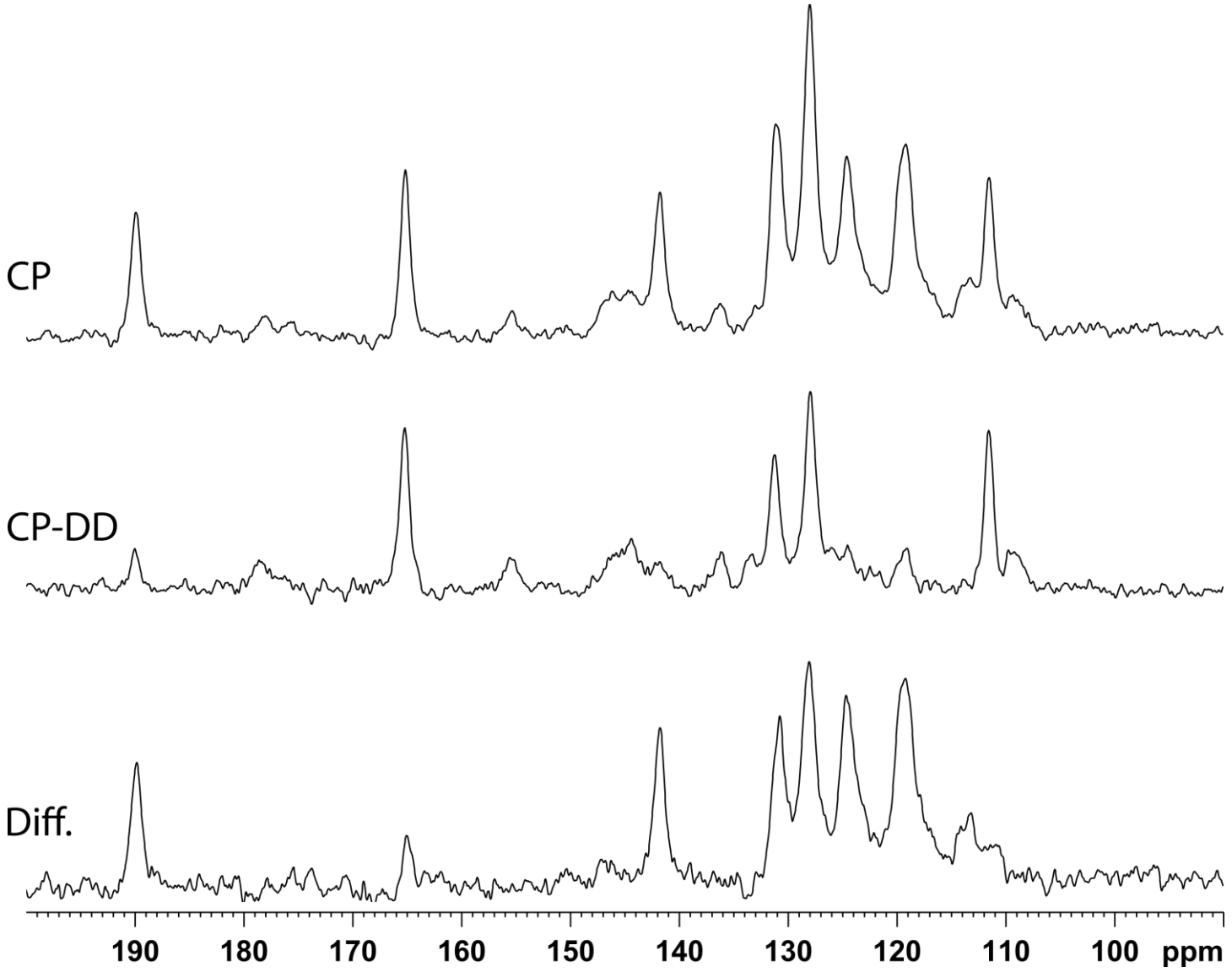

S4.5. $^{13}C\{^{1}H\}$CPMAS NMR spectrum of 3b

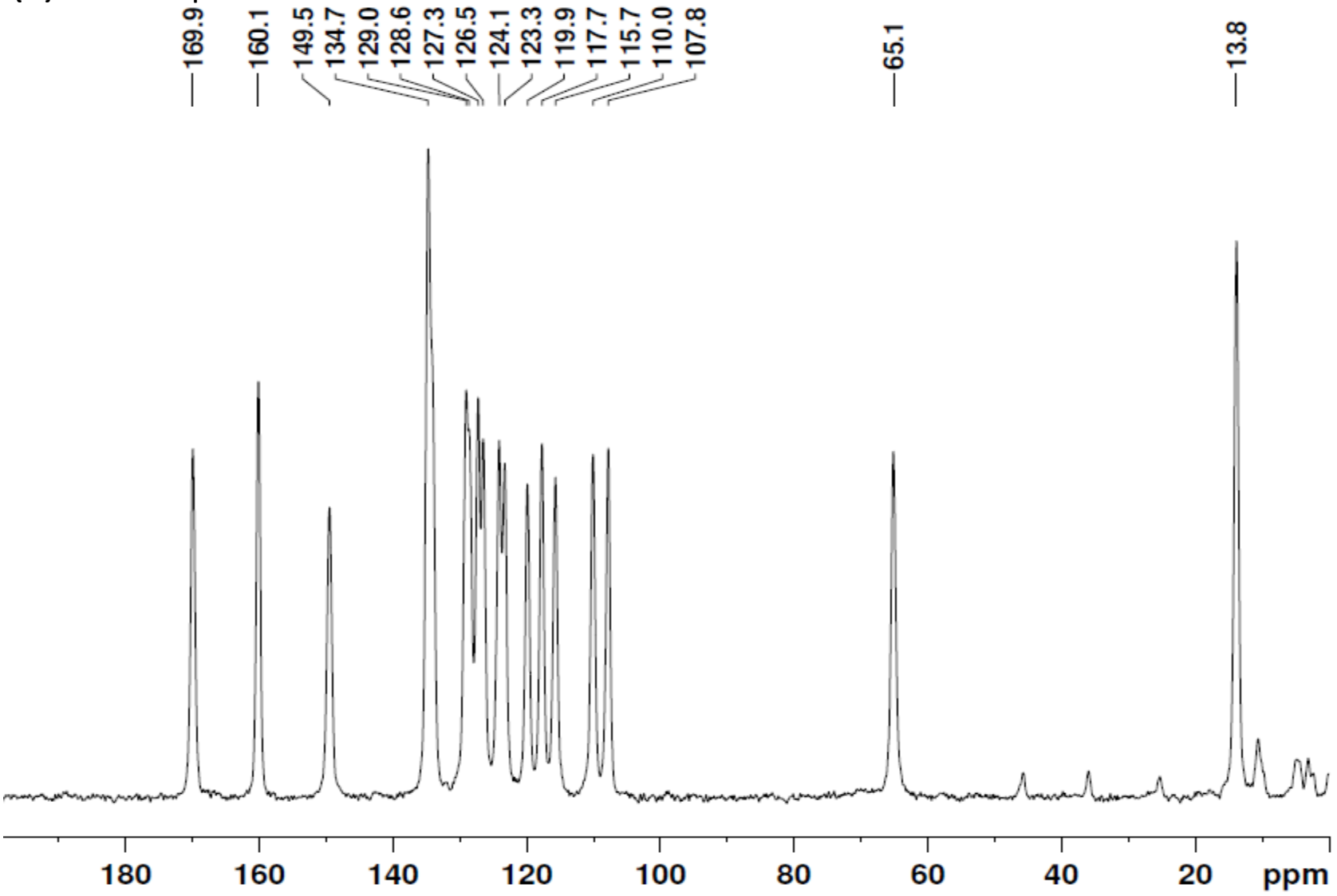

S4.6. Expansion of $^{13}C\{^{1}H\}$CPMAS NMR spectrum of 3b

With normal CP and dipolar dephasing (CP-DD)

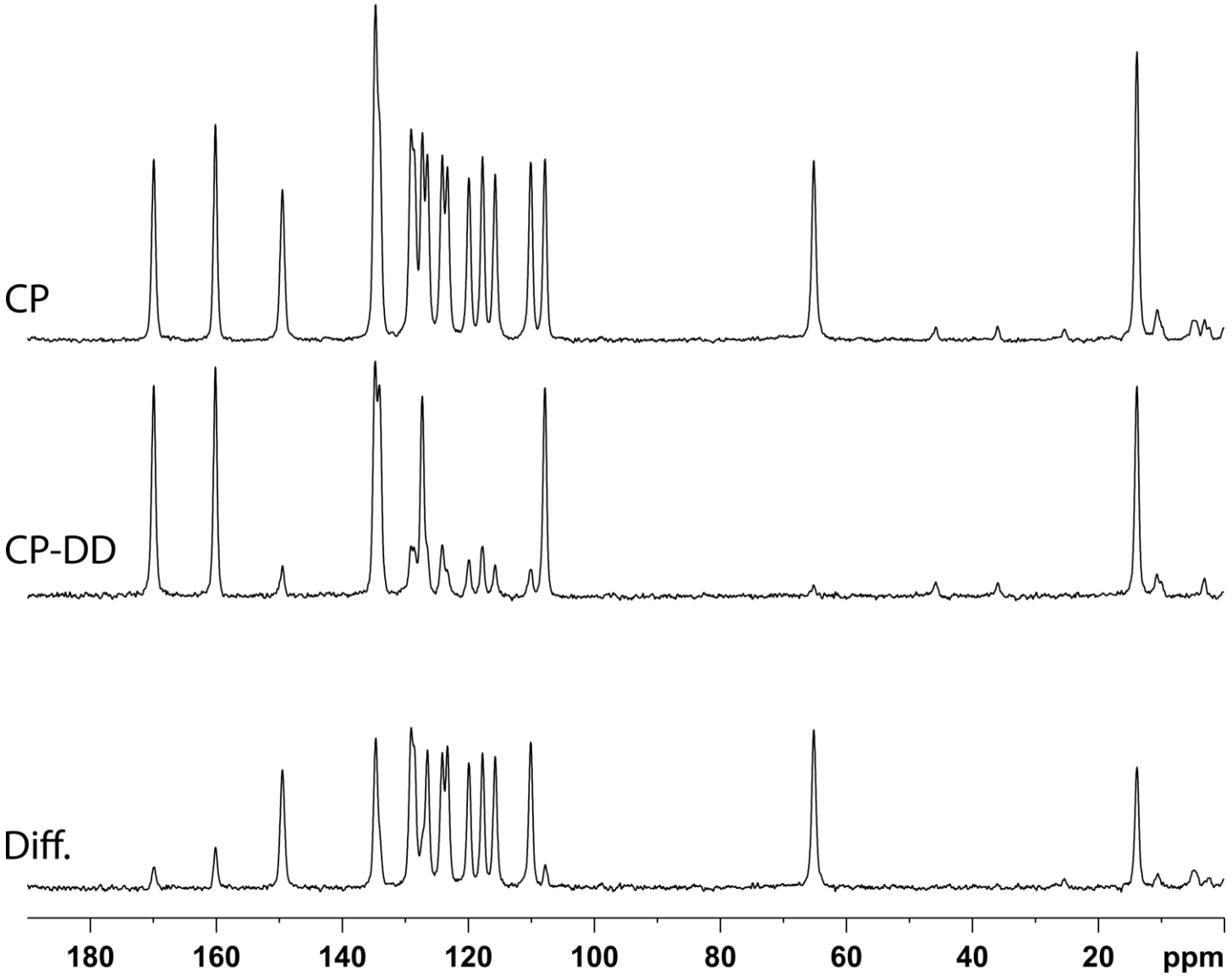

S4.7. $^{13}C\{^{1}H\}$**CPMAS NMR spectrum of 3c**

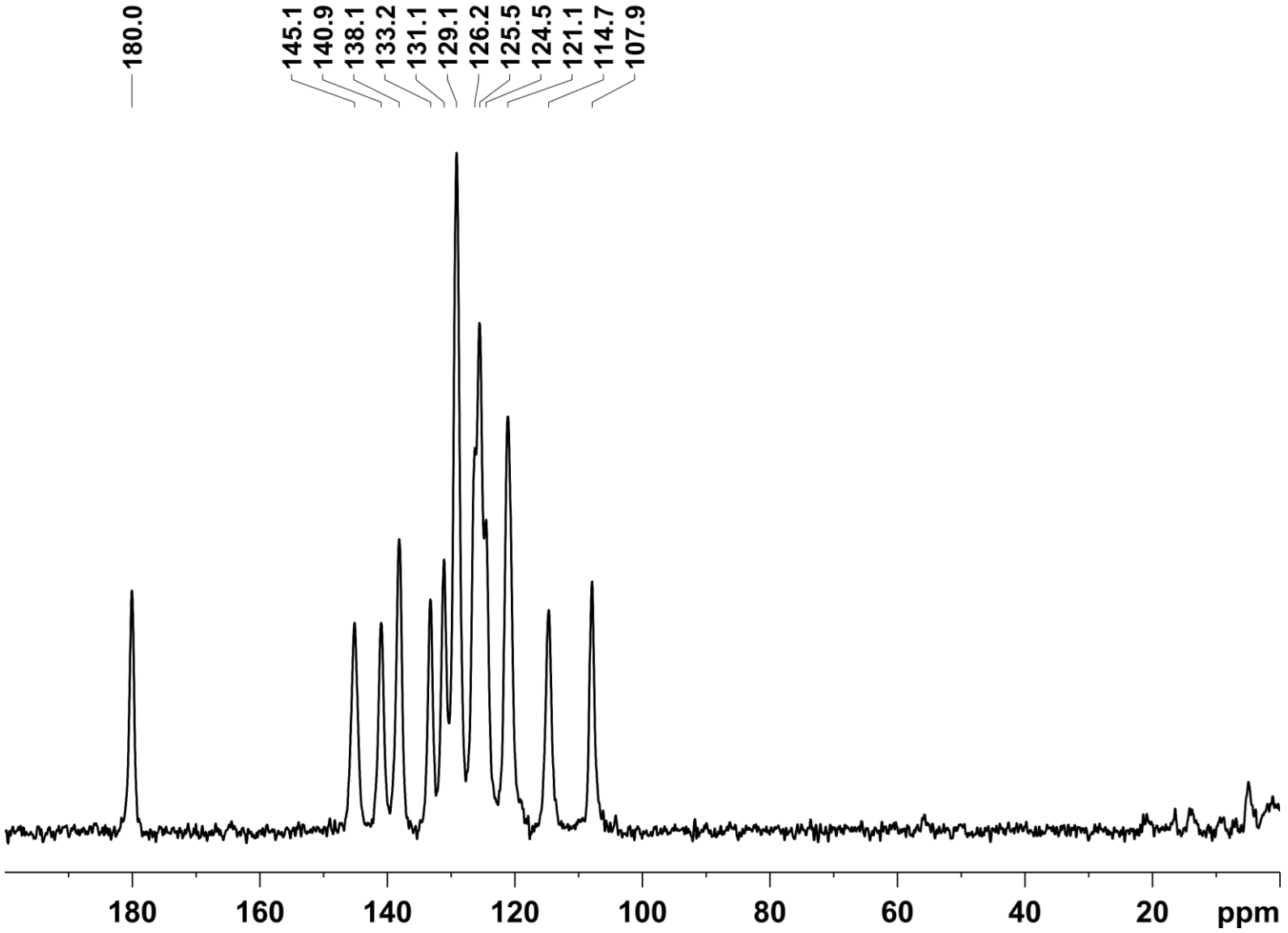

S4.8. Expansion of $^{13}C\{^{1}H\}$CPMAS NMR spectrum of 3c

With normal CP and dipolar dephasing (CP-DD)

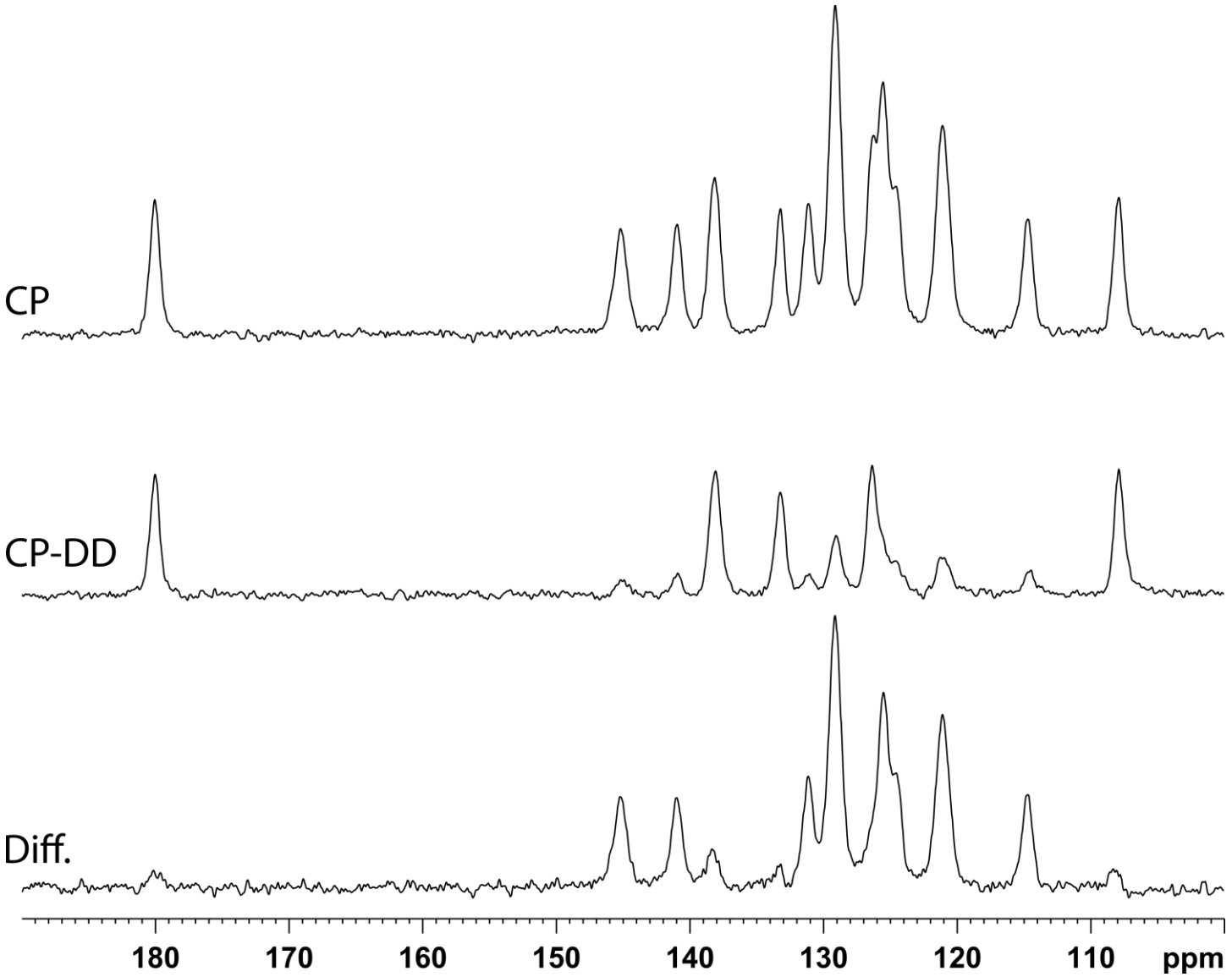

S4.9. $^{13}C\{^{1}H\}$CPMAS NMR spectrum of 3d

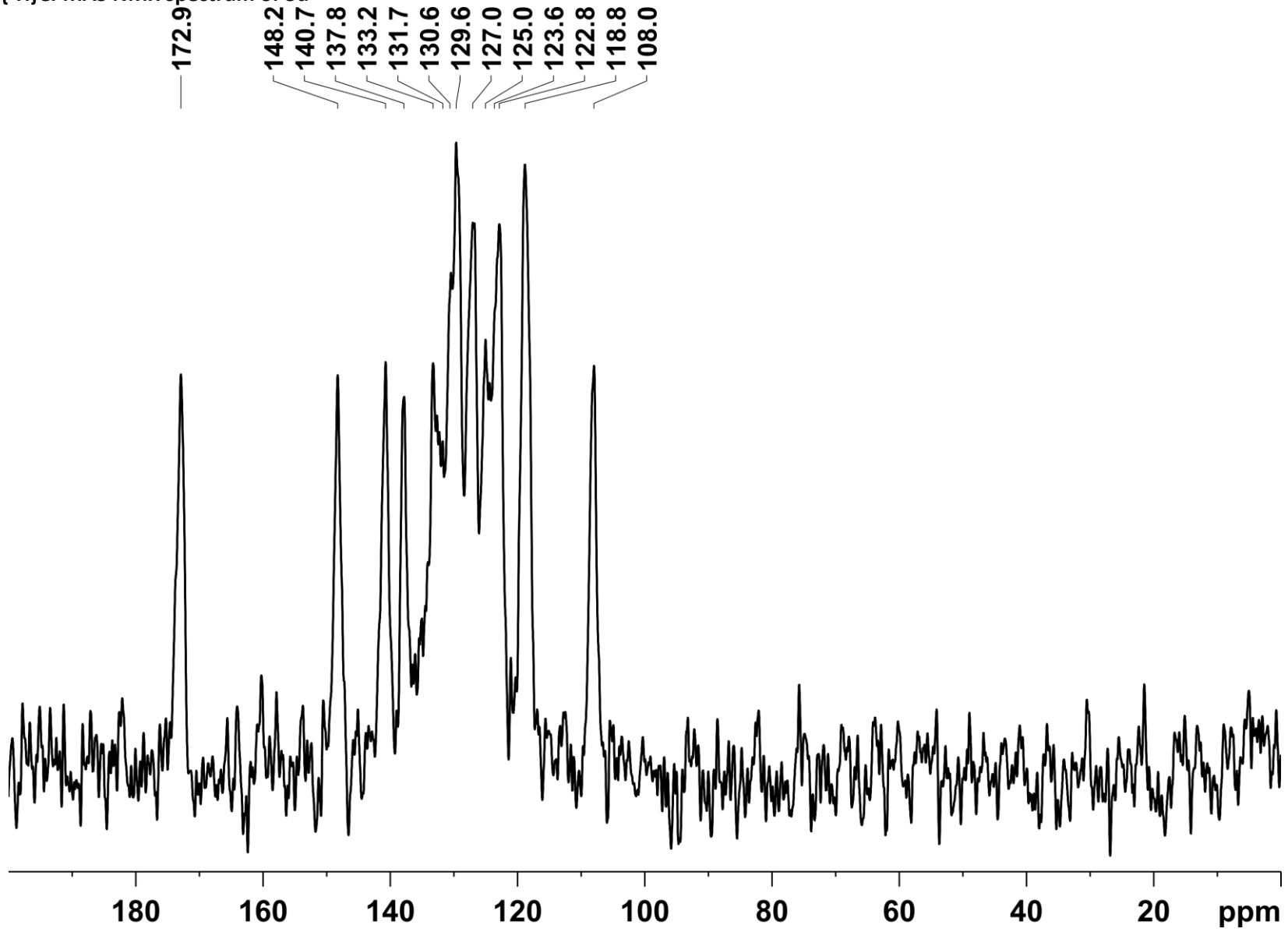

S4.10. $^{13}C\{^{1}H\}$CPMAS NMR spectrum of 3e

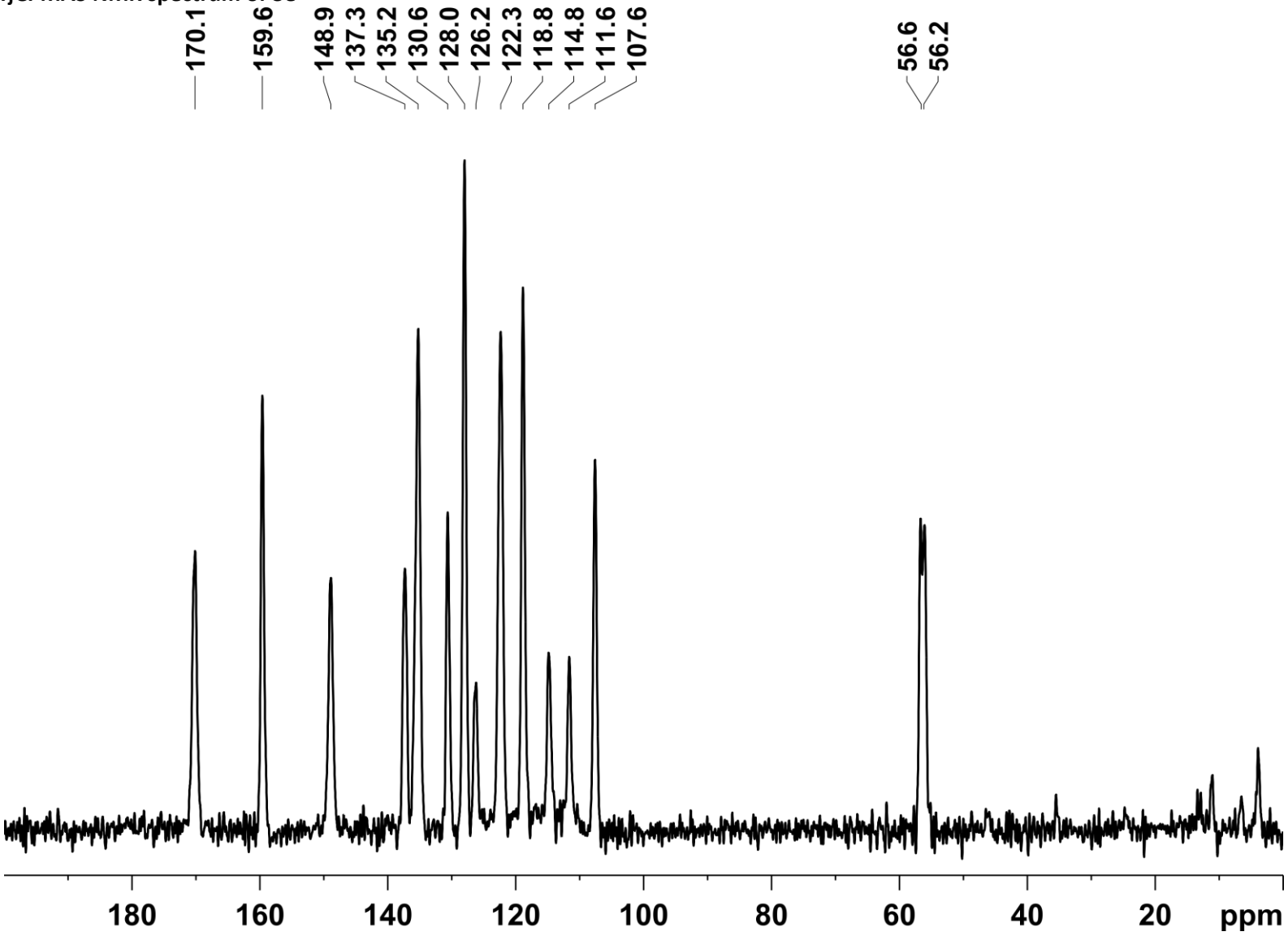

S4.11. Extension of $^{13}C\{^{1}H\}$CPMAS NMR spectrum of 3e

With normal CP and dipolar dephasing (CP-DD)

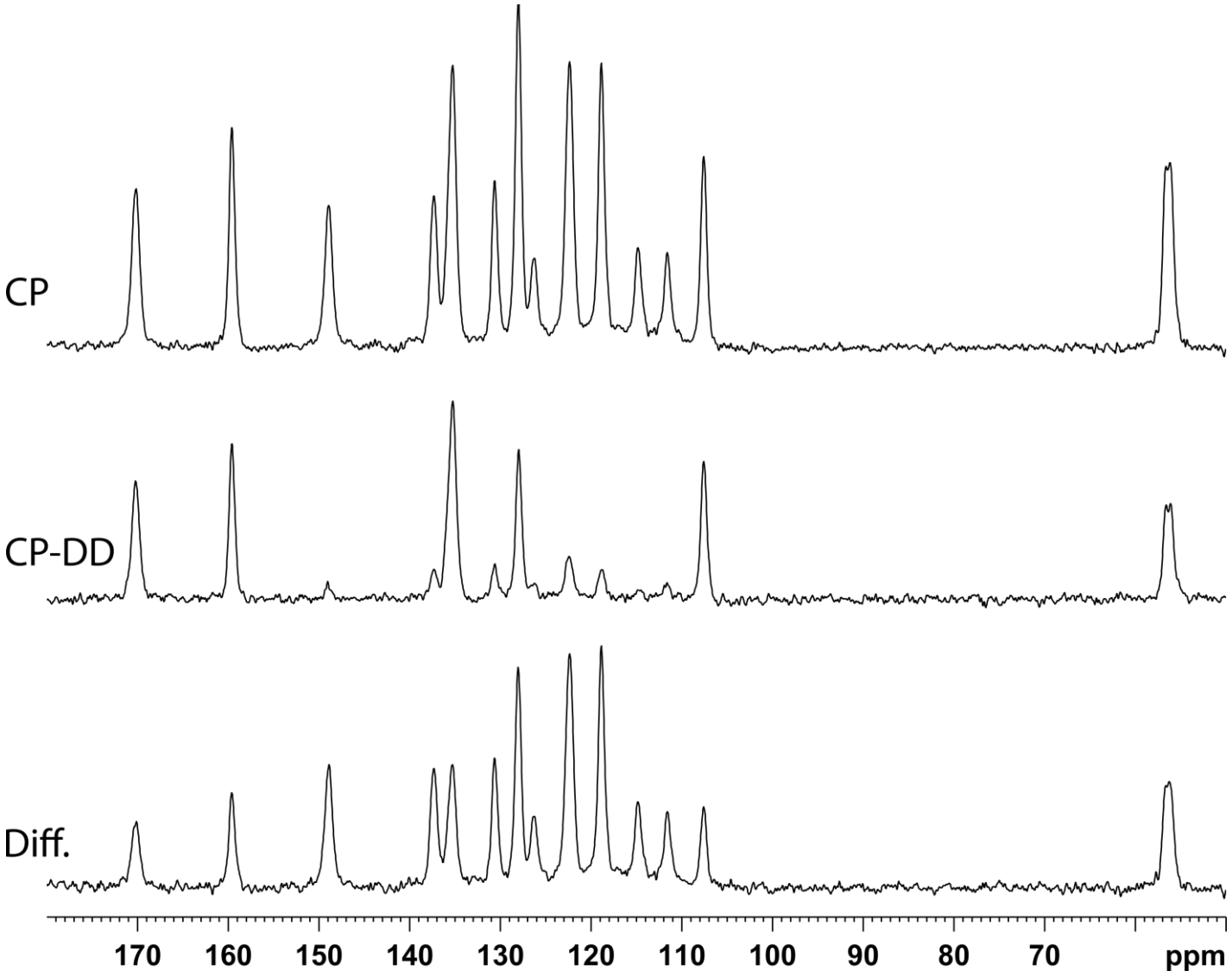

S4.12. ^{1}H NMR spectrum of 3a from the reaction of 1 with 2a

Recorded in CD_2Cl_2 solution, 399.78 MHz

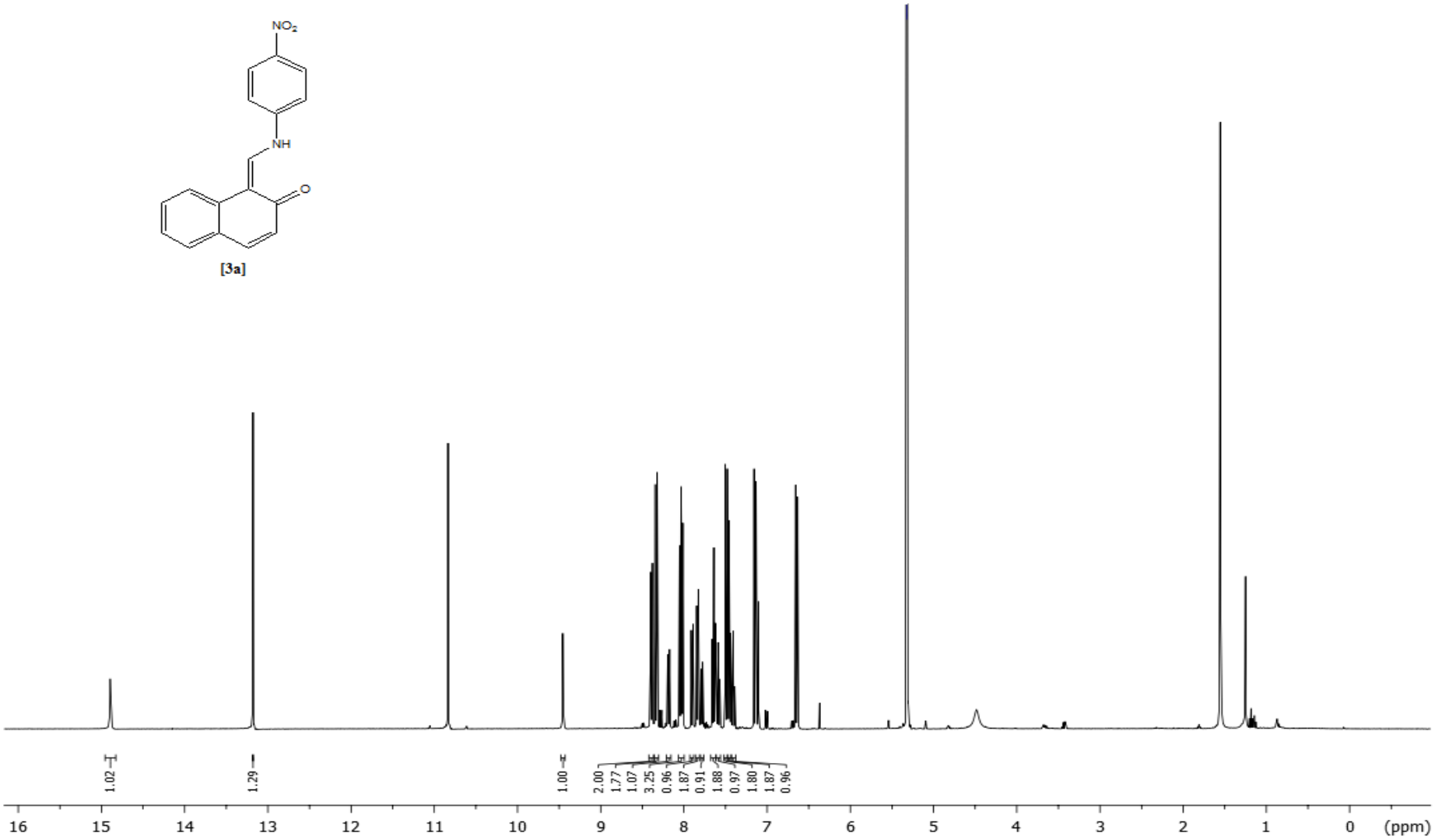

S4.13. ^{13}C NMR spectrum of 3a from the reaction of 1 with 2a

Recorded in CD_2Cl_2 solution, 100.53 MHz

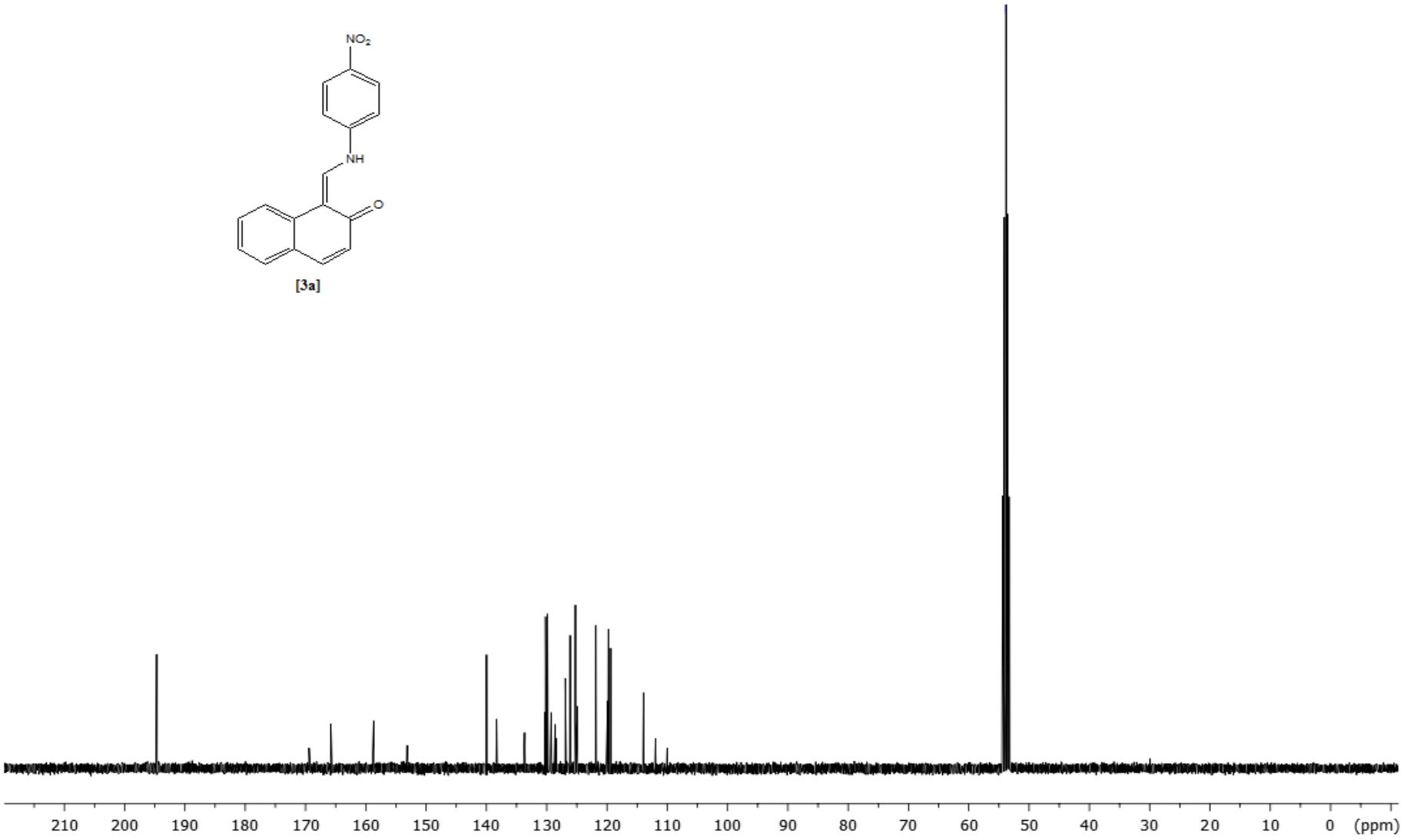

S4.14. ^{1}H NMR spectrum of 3b from the reaction of 1 with 2b

Recorded in CD_2Cl_2 solution, 399.78 MHz

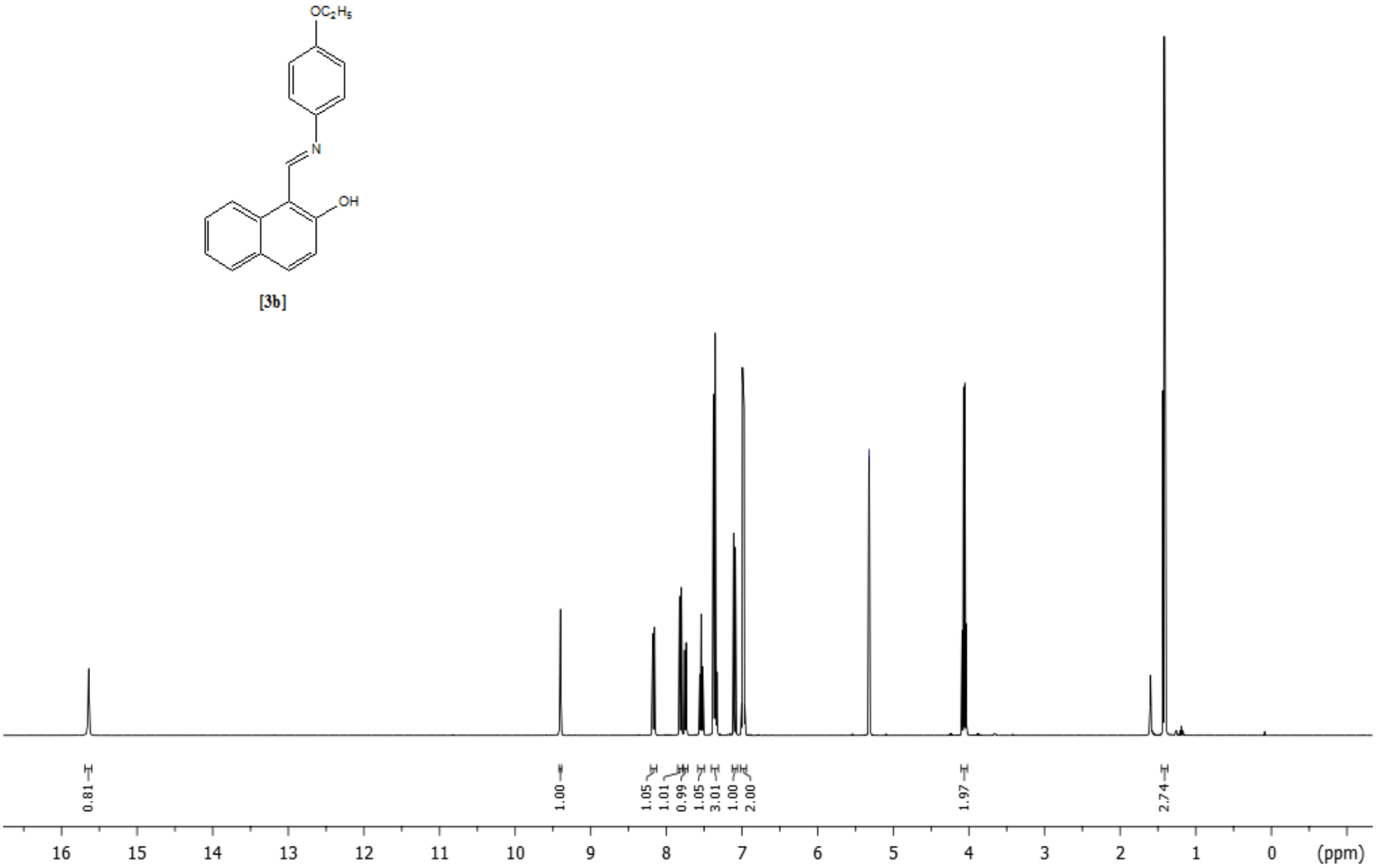

S4.15. ^{13}C NMR spectrum of 3b from the reaction of 1 with 2b

Recorded in CD_2Cl_2 solution, 100.53 MHz

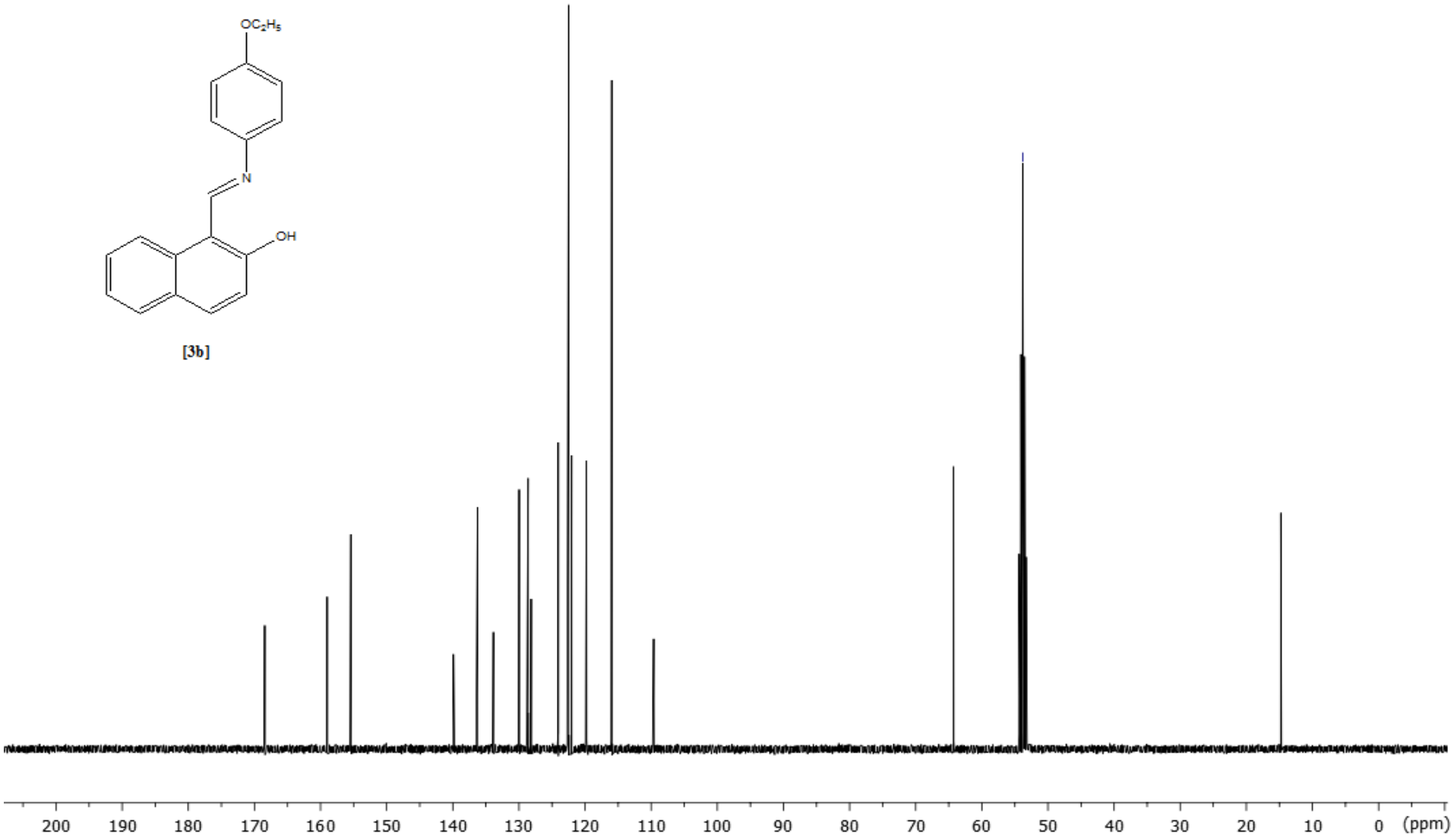

S4.16. ^{1}H NMR spectrum of 3c from the reaction of 1 with 2c

Recorded in CD_2Cl_2 solution, 399.78 MHz

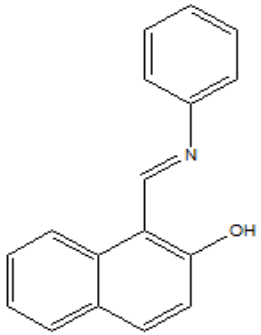

[3c]

S4.17. ^{13}C NMR spectrum of 3c from the reaction of 1 with 2c

Recorded in CD_2Cl_2 solution, 100.53 MHz

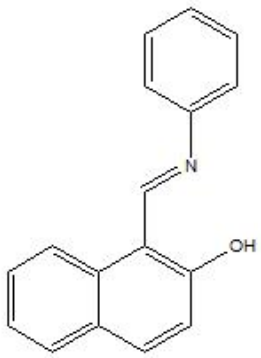

[3c]

S4.18. ^{1}H NMR spectrum of 3d from the reaction of 1 with 2d

Recorded in CD_2Cl_2 solution, 399.78 MHz

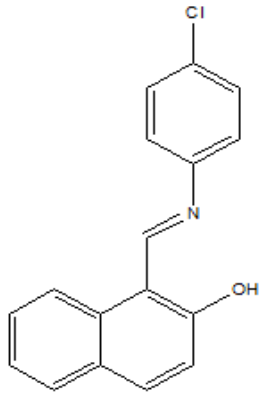

[3d]

S4.19. ^{13}C NMR spectrum of 3d from the reaction of 1 with 2d

Recorded in CD_2Cl_2 solution, 100.53 MHz

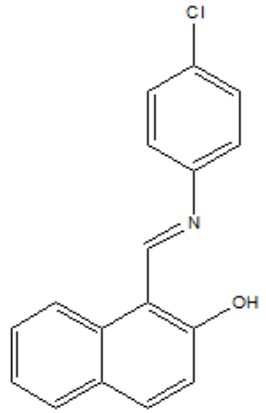

[3d]

S4.20. ^{1}H NMR spectrum of 3e from the reaction of 1 with 2e

Recorded in CD_2Cl_2 solution, 399.78 MHz

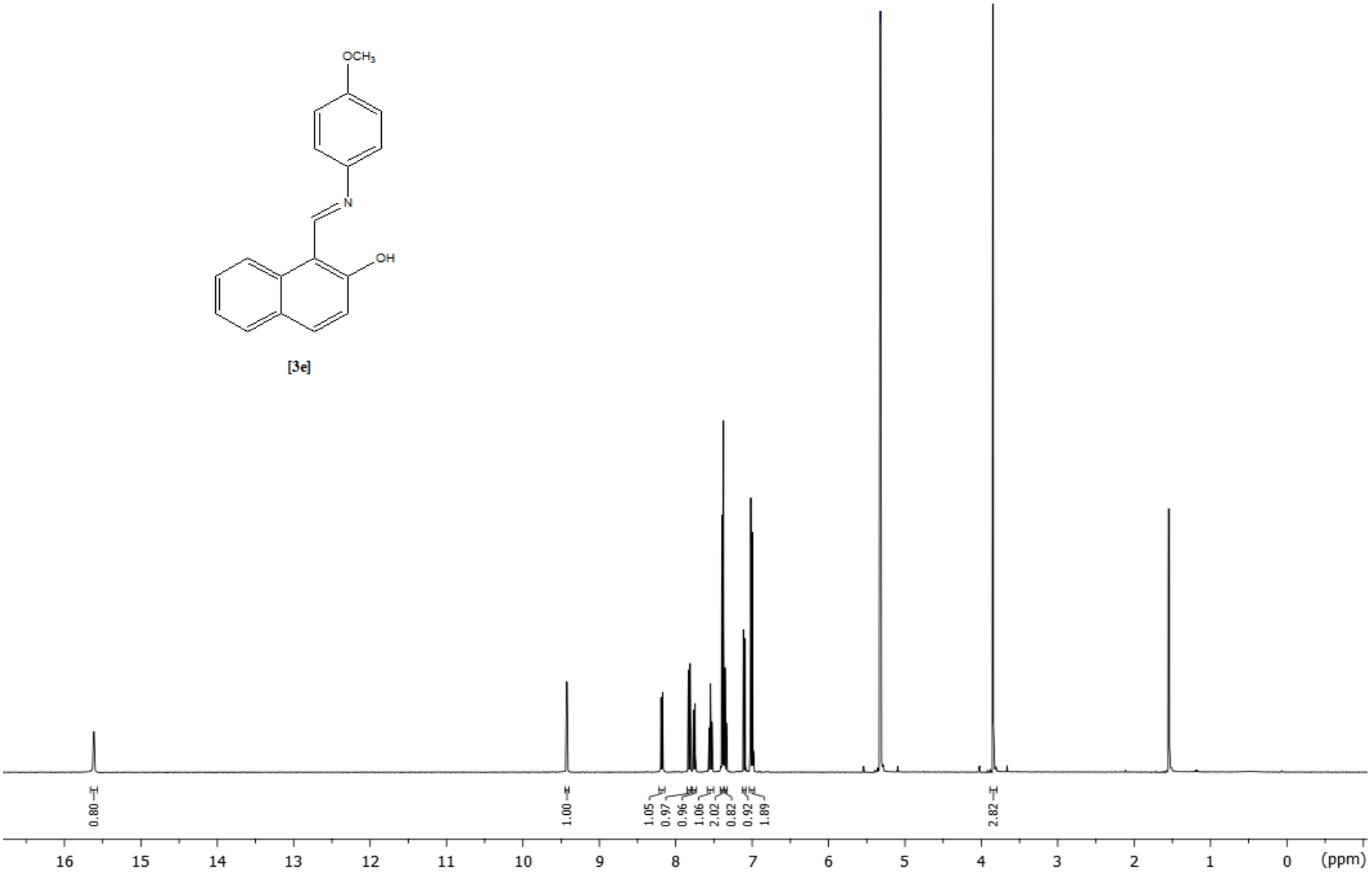

S4.21. ^{13}C NMR spectrum of 3e from the reaction of 1 with 2e

Recorded in CD_2Cl_2 solution, 100.53 MHz

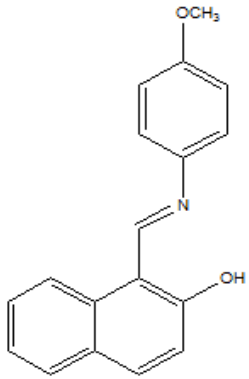

[3e]

S4.22. ^{1}H NMR spectrum of 4b-a and 4b-b

Recorded in CD_2Cl_2 solution, 399.78 MHz

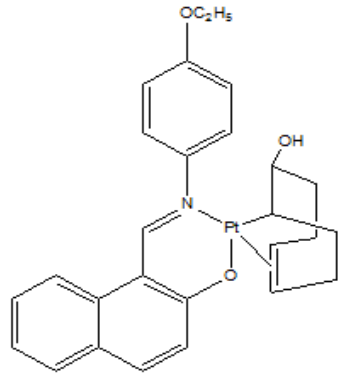

[4b-a]

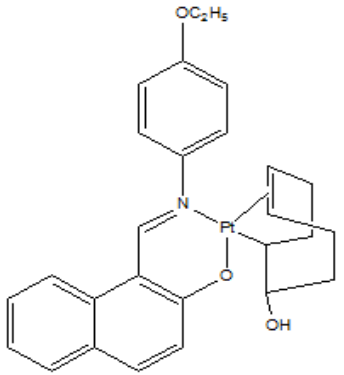

[4b-b]

S4.23. ^{13}C NMR spectrum of 4b-a and 4b-b

Recorded in CD_2Cl_2 solution, 100.53 MHz

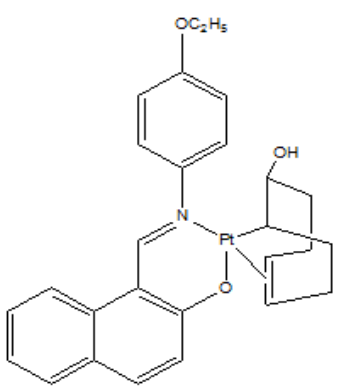

[4b-a]

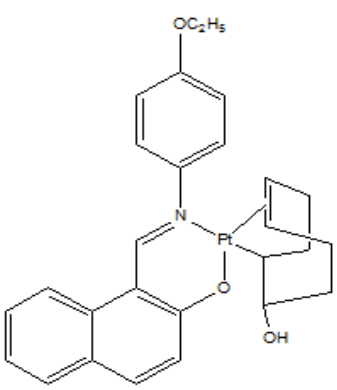

[4b-b]

S4.24. ^{1}H NMR spectrum of 4c-a and 4c-b

Recorded in $CDCl_3$ solution, 399.78 MHz

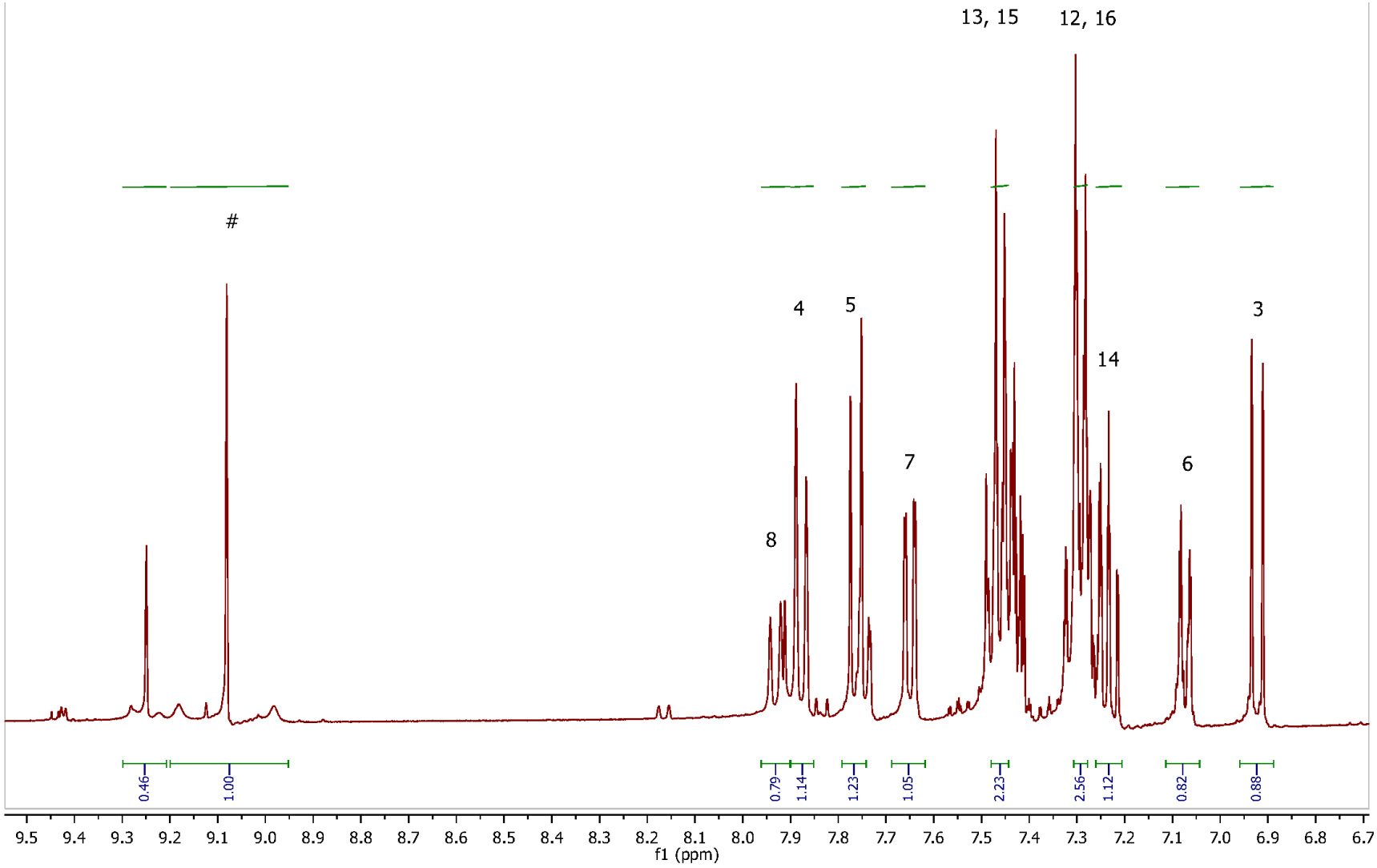

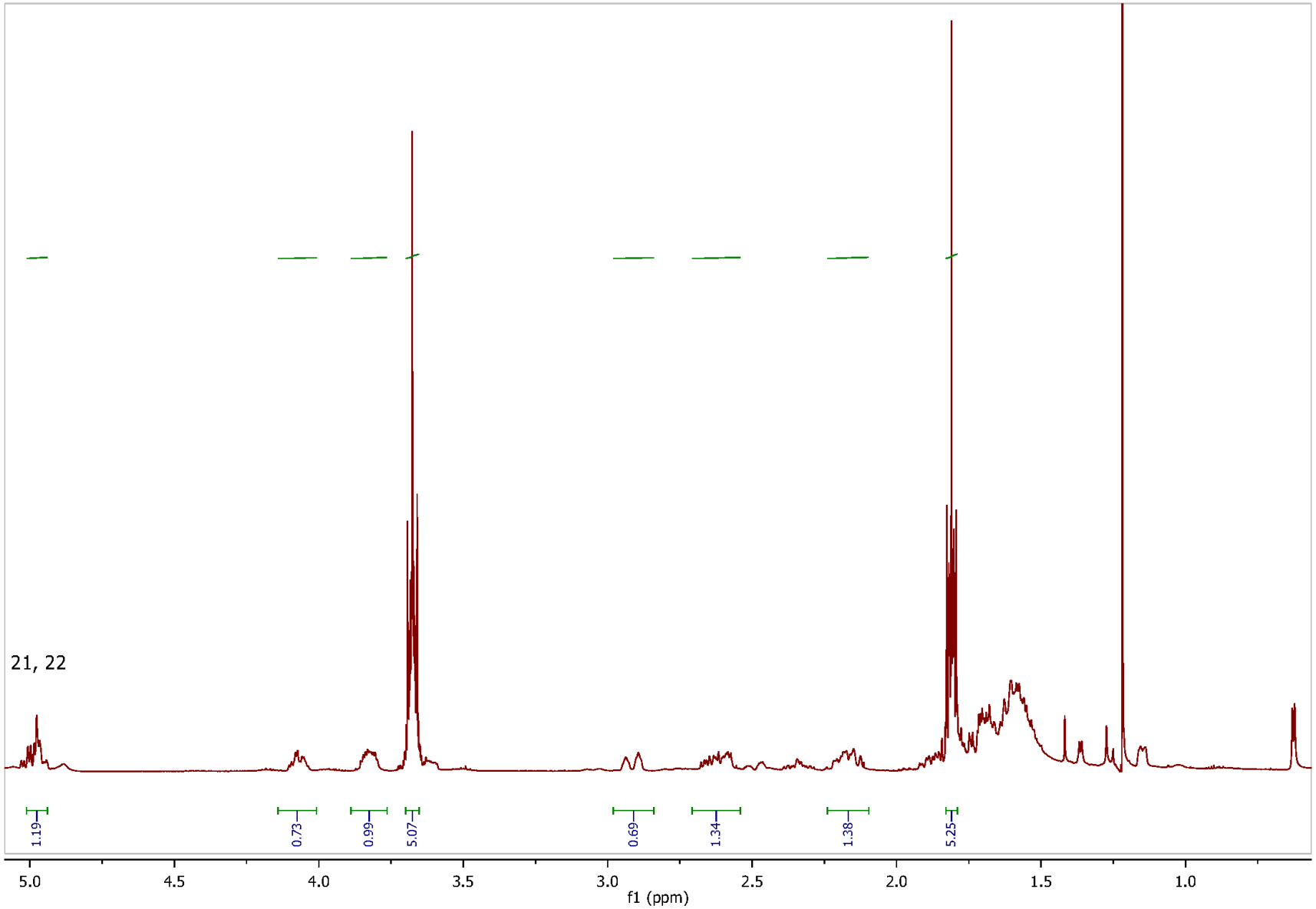
21, 22
1.19
0.73
0.99
5.07
0.69
1.34
1.38
5.25
5.0
4.5
4.0
3.5
3.0
2.5
2.0
1.5
1.0
f1 (ppm)

S4.25. ^{13}C NMR spectrum of 4c-a and 4c-b

Recorded in CD_2Cl_2 solution, 100.53 MHz

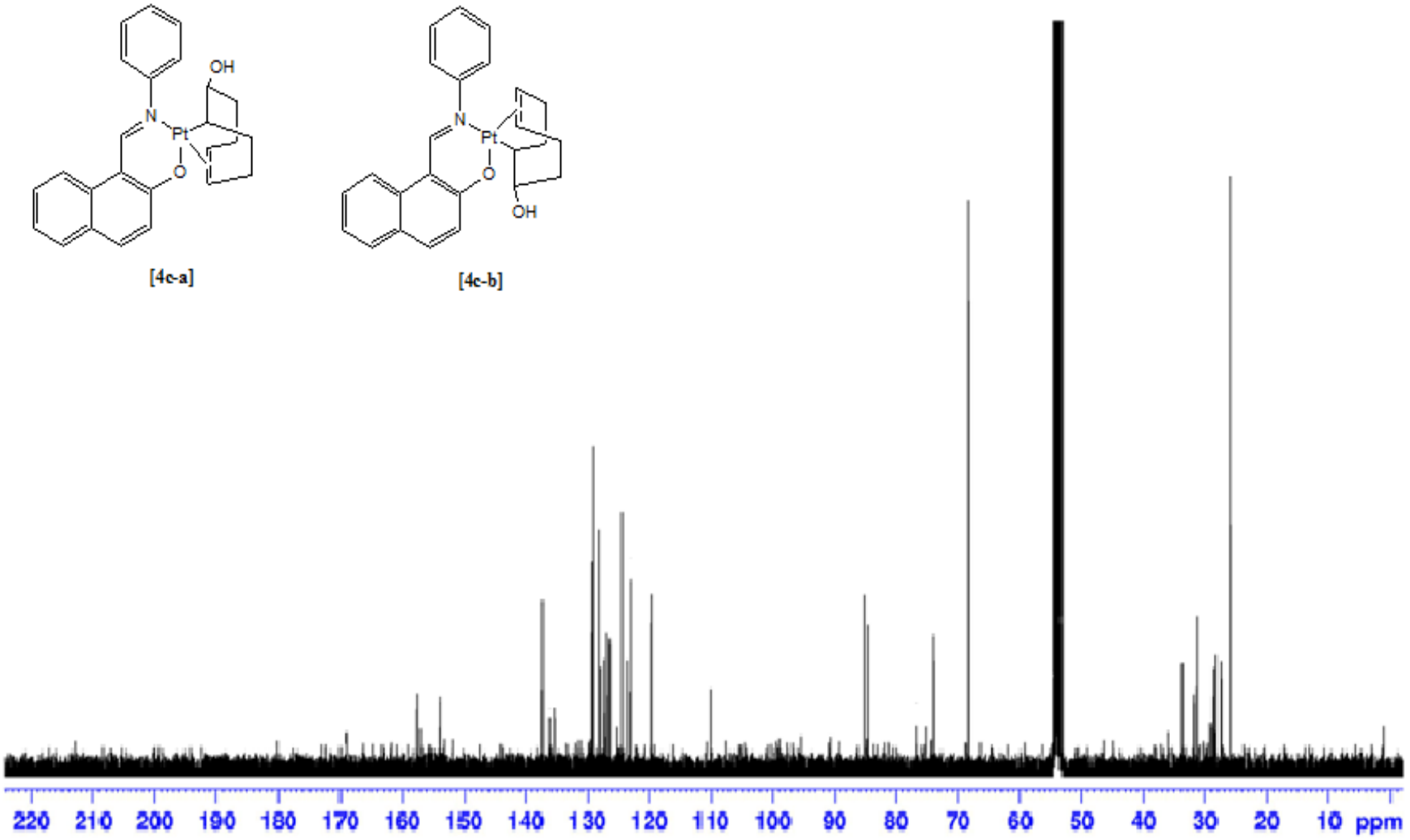

S4.26. ^{1}H NMR spectrum of 4d-a and 4d-b

Recorded in CD_2Cl_2 solution, 399.78 MHz

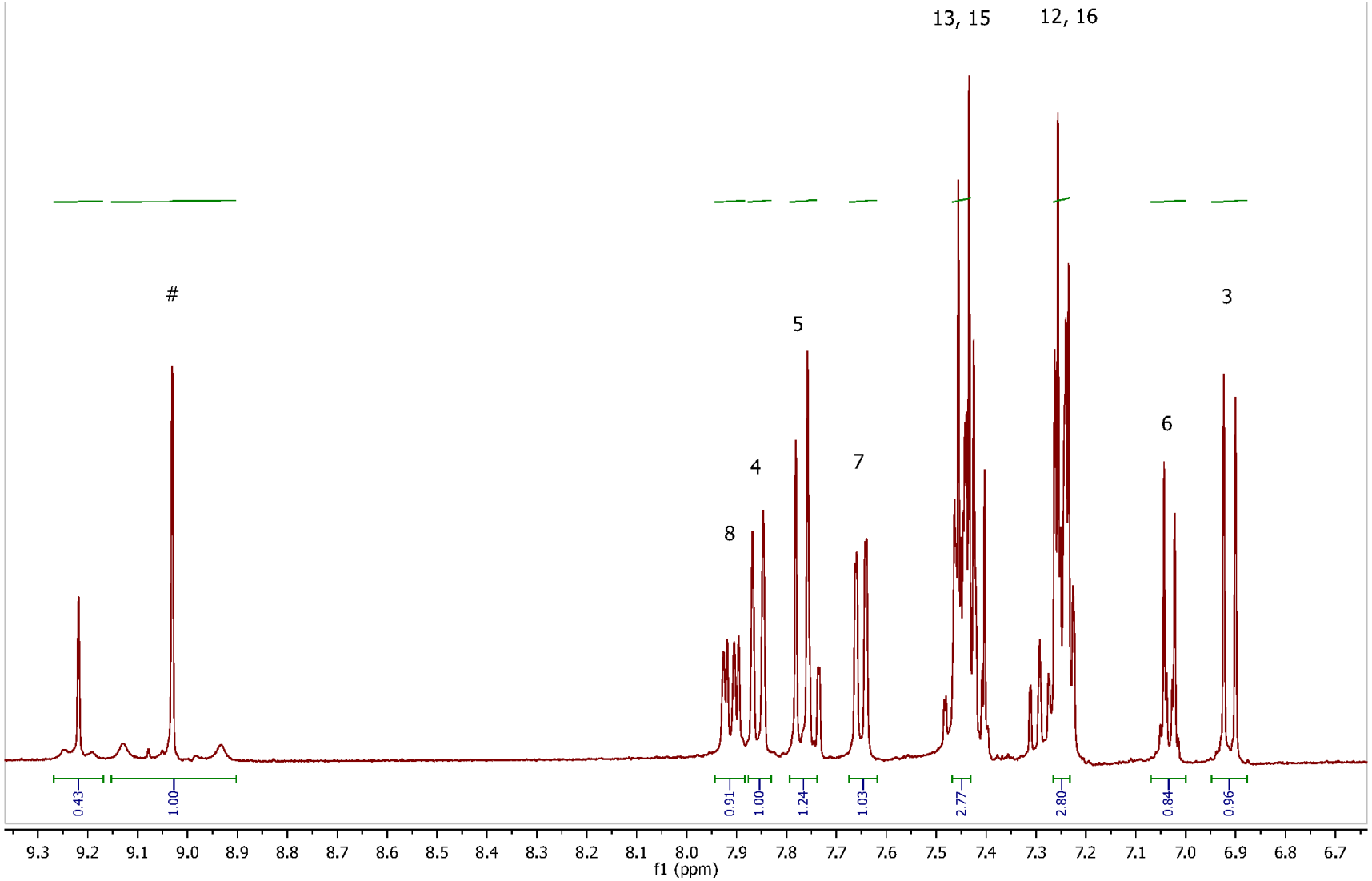

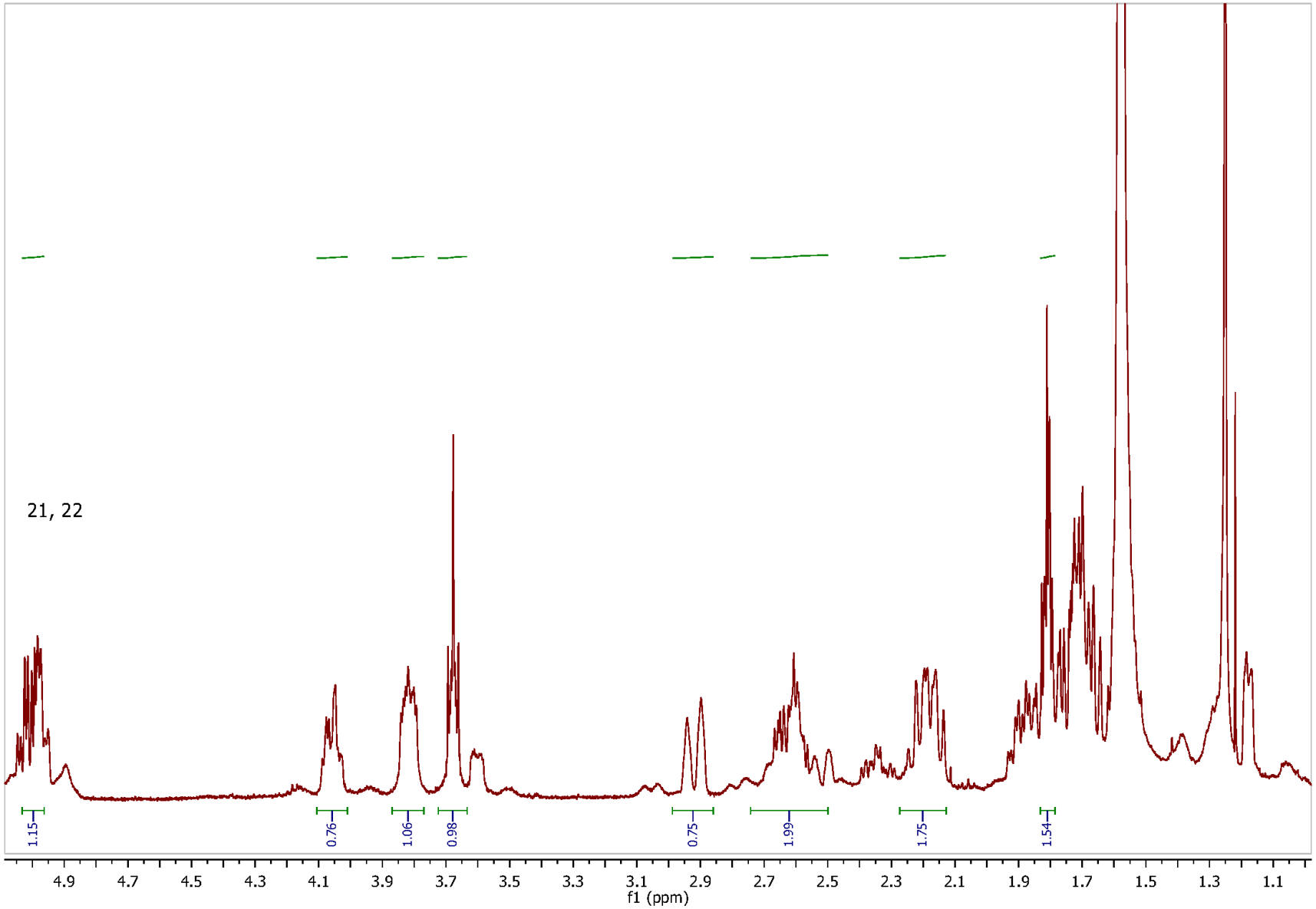
21, 22
1.15
0.76
1.06
0.98
0.75
1.99
1.75
1.54
4.9
4.7
4.5
4.3
4.1
3.9
3.7
3.5
3.3
3.1
2.9
2.7
2.5
2.3
2.1
1.9
1.7
1.5
1.3
1.1
f1 (ppm)

S4.27. ^{1}H NMR spectrum of 4e-a and 4e-b

Recorded in CD_2Cl_2 solution, 399.78 MHz

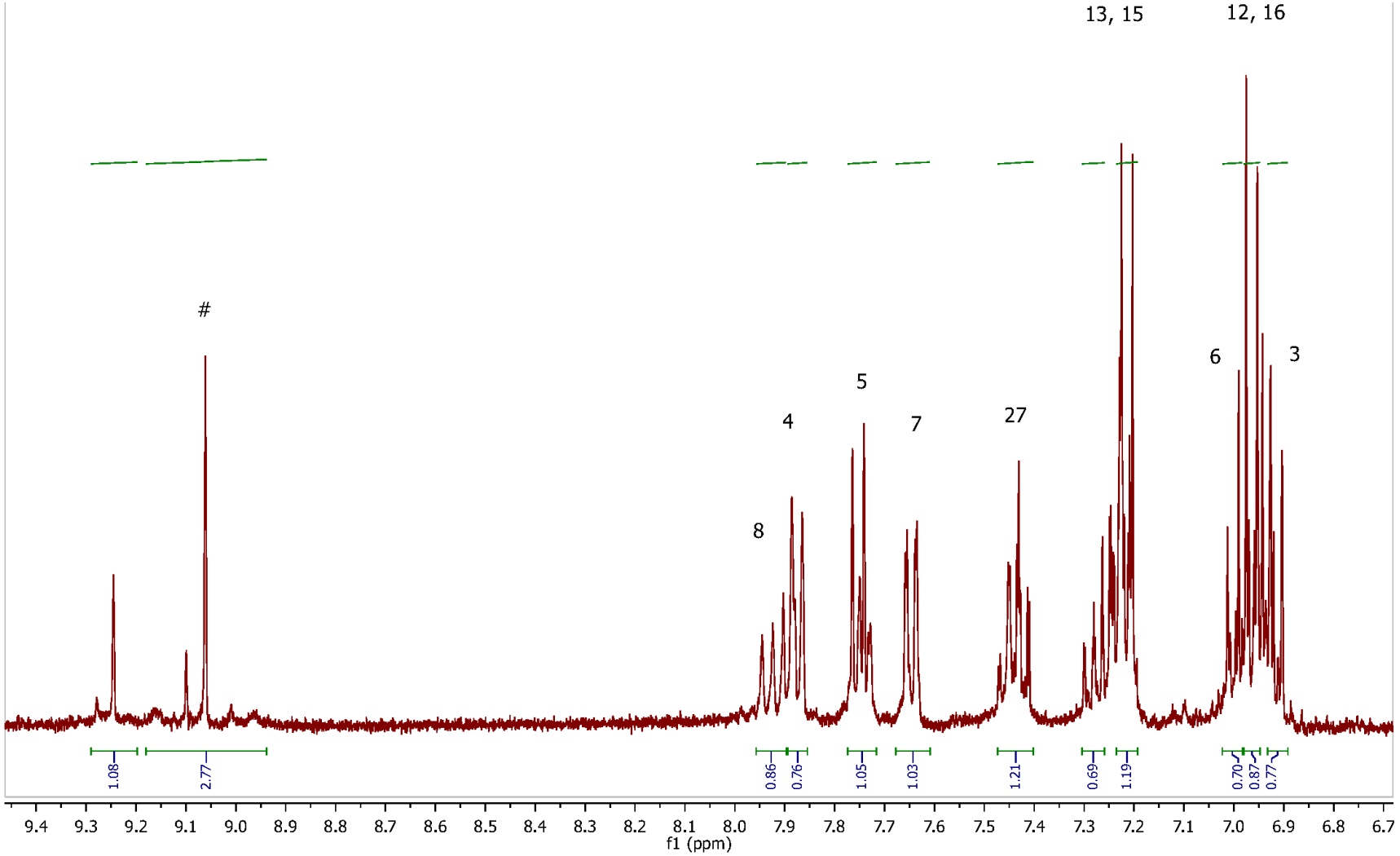

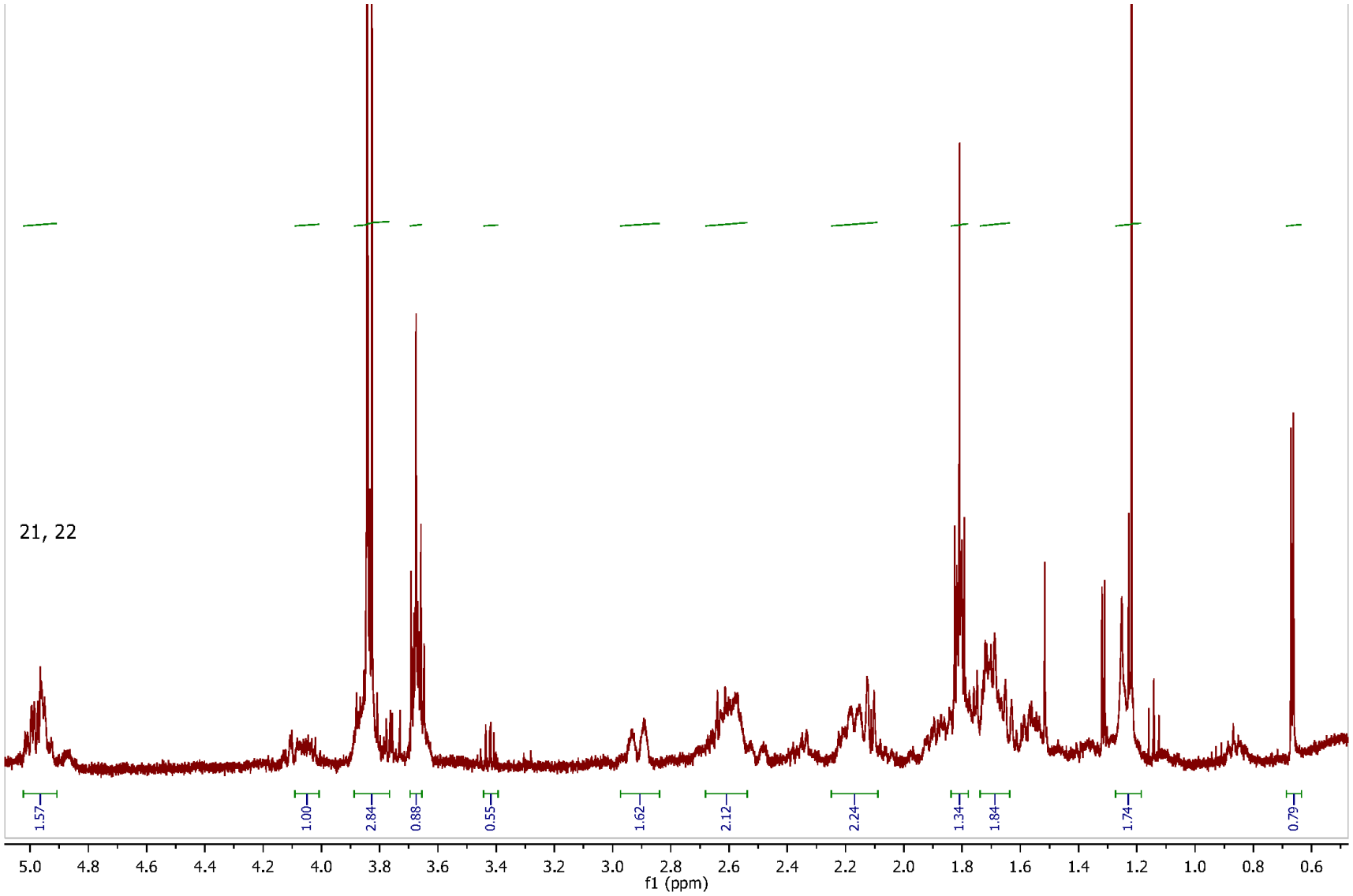
21, 22
1.57
1.00
2.84
0.88
0.55
1.62
2.12
2.24
1.34
1.84
1.74
0.79
5.0
4.8
4.6
4.4
4.2
4.0
3.8
3.6
3.4
3.2
3.0
2.8
2.6
2.4
2.2
2.0
1.8
1.6
1.4
1.2
1.0
0.8
0.6
f1 (ppm)

S4.28. ^{13}C NMR spectrum of 4e-a and 4e-b

Recorded in CD_2Cl_2 solution, 100.53 MHz

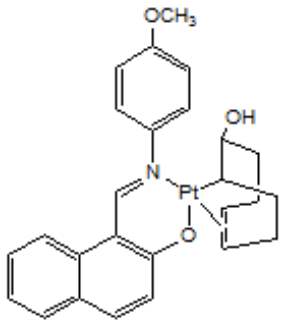

[4e-a]

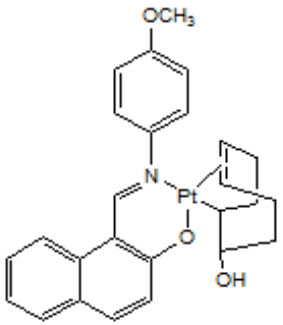

[4e-b]

S5. References

(1) *CrysAlisPro, Oxford Diffraction Ltd. Version 1.171.34.40*.

(2) *Empirical absorption correction using spherical harmonics, implemented in SCALE3 ABSPACK scaling algorithm within CrysAlisPro software, Oxford Diffraction Ltd. Version 1.171.34.40*.

(3) Dolomanov, O. V.; Blake, A. J.; Champness, N. R.; Schroder, M. *J. Appl. Crystallogr.* **2003**, *36*, 1283.

(4) (a) Palatinus, L.; Chapuis, G. *J. Appl. Crystallogr.* **2007**, *40*, 786;(b) Palatinus, L.; van der Lee, A. *J. Appl. Crystallogr.* **2008**, *41*, 975;(c) Palatinus, L.; Prathapa, S. J.; van Smaalen, S. *J. Appl. Crystallogr.* **2012**, *45*, 575.

(5) Sheldrick, G. M. *Acta Crystallogr. Sect. A* **2008**, *64*, 112.

(6) (a) Duisenberg, A. J. M. *J. Appl. Crystallogr.* **1992**, *25*, 92;(b) Duisenberg, A. J. M.; Hooft, R. W. W.; Schreurs, A. M. M.; Kroon, J. *J. Appl. Crystallogr.* **2000**, *33*, 893.